Research and Development Progress Report No. 594 • December 1970

The Structure and Morphology of Inorganic Membranes

By W. O. Milligan, M. Uda, M. L. Beasley, Dennis R. Dillin, Wayne E. Bailey and J. J. McCoy, Baylor University, Waco, Texas, for Office of Saline Water, Chung-ming Wong, Director; W. Sherman Gillam, Assistant Director, Research; Lee Leiserson, Chief, Chemistry Division

Grant No. 14–01–0001–1296

UNITED STATES DEPARTMENT OF THE INTERIOR • Walter J. Hickel, Secretary
Carl L. Klein, Assistant Secretary for Water Quality and Research

For sale by the Superintendent of Documents, U.S. Government Printing Office, Washington, D.C. 20402 - Price 75 cents

TABLE OF CONTENTS

I. INTRODUCTION 1
II. HISTORICAL BACKGROUND 2
A. *Definitition of Semi-Permeable Membrane* 2
B. *Mechanisms of Semi-Permeability* 2
C. *Water Content of Cupric Ferrocyanide Gels* 8
D. *X-Ray Diffraction Studies* 10
E. *Electron Diffraction Studies* 11
III. SEMI-PERMEABILITY 11
IV. STRUCTURE AND MORPHOLOGY OF HEAVY METAL CYANO COMPLEXES ... 12
A. *Cubic Ferro-, Ferri-, and Cobalti-cyanides* 12
1. EXPERIMENTAL 12
a. Preparation of Samples 12
b. Dehydration Isobars 13
c. Densities 14
d. X-ray Diffraction 14
e. Intensity Calculations 14
2. RESULTS AND CONCLUSIONS 15
a. Dehydration Isobars 15
b. Lattice Constants and Densities 17
c. Parameters and Temperature Factors 20
d. Interatomic Distances 25
B. *Hexagonal Ferro- and Ferri-cyanides* 29
C. *Aging Effects in Cupric Ferrocyanide* 34
1. EXPERIMENTAL 34
a. Preparation of Samples 34
b. Electron Microscopy 35
c. Electron Diffraction 36
d. Low Angle Electron Diffraction 36
2. RESULTS AND CONCLUSIONS 36
a. Freshly Precipitated Cupric Ferrocyanide 36
b. Aging Under Water at Room Temperature 39
c. Aging Under Water at 100° C 39
d. Water Content of Cupric Ferrocyanide 39
e. Cupric Ferrocyanide Sheets 42
f. Dehydration-Rehydration Isobars 43
g. X-ray Diffraction 47
h. Cupric Ferrocyanide Free of Sheet-Like Morphology 47
i. Orientation Effects 48
j. Acceleration of Aging in Acids 50
k. Evacuation Effects 51
V. EFFECT OF RADIUS RATIO AND DOUBLE REPULSION 56

ABSTRACT

The structure and morphology of the classic semi-permeable membrane, cupric ferrocyanide, and some 40 other heavy metal ferro-, ferri-, and cobalti-cyanides have been studied by isobaric dehydration, x-ray and electron diffraction, low angle electron diffraction, infra-red, and Mössbauer spectroscopy.

Freshly precipitated cupric ferrocyanide gel is composed of 10 Å amorphous particles, which age under water to become crystalline (Fm3m, a_o = 10.013 ± 0.001 Å) within 10 to 15 minutes. After about 20 hours, platelike particles appear, exhibiting new diffraction lines corresponding to a larger cubic unit cell (a_o = *ca* 20 Å), and yielding a step-wise dehydration isobar corresponding to $H_2O/Cu_2Fe(CN)_6$ = *ca* 8. In the absence of the plates, $Cu_2Fe(CN)_6$ exhibits a bivarient dehydration isobar like some 30 other cyanide complexes studied here. Additional large x-ray spacings not identical with those of $Cu_2Fe(CN)_6$, and color changes on dehydration have been observed for well-aged $Co_3[Fe(CN)_6]_2$ (blue → reddish-violet), $Ni_3[Co(CN)_6]_2$ (blue → green), and $Co_3[Co(CN)_6]_2$ (rose →blue). For cations of "crystal radius" less than about 1 Å, heavy metal cyanide complexes are cubic (unit cell dimensions are reported for about 30 such). For radii over 1 Å, the crystals are hexagonal (La, Pr, Nd, Bi, Th, etc. are reported here). Large single crystals of $LaFe(CN)_6$ are described. Carbon-nitrogen distances (1.148 to 1.160 Å for some 30 compounds) derived from x-ray intensity calculations correlate with observed infra-red CN stretching frequencies and cubic lattice constant sequences.

The pore structure of heavy metal cyanide complexes consists of the interstices between spheroidal or platelike particles. The morphology is more significant than the particle size. Hydrated cupric ferrocyanide is unique in forming sheets, assumed to be the active semi-permeable structure, water being transported through the channel-like interstices, regular in this case, but irregular in membranes composed of spheroidal particles.

I. INTRODUCTION

Since the phenomenon of osmosis was recognized and utilized in dialysis and separations, first in the separation of colloids from material in true solution and later in the selective separation of ions and molecules in solution, numerous investigations have been made in the general field of membrane equilibria. In biochemistry it has been recognized that all living cells are surrounded by a semi-permeable membrane. It has become increasingly important that the

a given membrane could be very impermeable to one or more other substances composed of larger molecules. The sieve theory cannot explain the lack of diffusion of water through latex membranes, although larger molecules such as benzene and pyridine diffuse very readily.

What is now designated as the *solution theory* was first discussed by Liebig (7,8) who said (7) in 1848 that:

> *"The volume changes of two miscible liquids separated from each other by a membrane depends upon the unequal wetting or attraction which the membrane exerts on the two liquids."*

Seven years later, L'hermite (9) carried out experiments intended to throw light on the solution theory. He placed in a test tube a layer of water, a thin layer of castor oil, and, finally, a layer of alcohol. After several days of standing, some of the alcohol had diffused through the separating layer of castor oil into the bottom water layer. L'hermite decided from this experiment and numerous other similar experiments that substances passing through a membrane must first dissolve in them. Kahlenberg (6) reported similar experiments where benzene and pyridine diffused through rubber, whereas water would not diffuse. Nernst (10) demonstrated that an animal membrane saturated with water was permeable to ether but not to benzene. Although the above cited experiments, as well as many others, strongly suggest the solution theory has some merit, Hartsung (11) pointed out that it is not easy to understand how a liquid can dissolve in a membrane without some of the membrane being dissolved in the liquid. Furthermore, Bigelow (12) and Bartell (13) demonstrated that osmotic effects can be observed with inert materials, such as a porous cup, where solution or chemical reaction with the liquid is unlikely. Gold or silver powder compressed into discs can exhibit some semi-permeable action.

Mathieu (14) observed that porous clay plates, certain animal membranes, parchment paper, and capillary space in tubes were capable of adsorbing more solvent than solute. This phenomenon has been designated as negative adsorption. Mathieu said that when membranes or capillaries are immersed in salt solutions, the liquid in the pore space will be a very diluted solution, or even in the extreme case of very fine pores, the space may contain solvent only. Thus, it appears reasonable that such membranes will be permeable only to the solvent. The *negative adsorption* theory was discussed by Nathansohn (15), Bancroft (16), and Tinker (17). The latter (17) found that cupric ferrocyanide membranes were impermeable to sugar. The size of the sugar molecule is not the significant factor, inasmuch as the

(*i.e.*, "hyperfiltration" or "reverse osmosis") membranes, that by neglecting interfacial effects, the effectiveness of membranes for separation of salts from water would presumably be determined either by the relative distribution of salts and the water between the solutions and the membrane phases or by differences in the relative transport properties (diffusion coefficients) of salts and water in the membrane phase or by a combination of both effects.

Furthermore, Kraus and co-workers (20) state that with uncharged membranes (*i.e.*, membranes not of the ion-exchange type) such as cellulose acetate membranes, that forces effecting either a difference in distribution of salts and water or a difference in their relative transport properties must be of short range. The effective portion of such hyperfiltration membranes thus has substantially the properties of homogenous aqueous—organic mixtures rather than a porous body. Also Kraus points out that the effectiveness of existing cellulose acetate membranes must be caused by an "effective layer" which has a low water content. He speaks of an "effective layer" of the membrane because it is now certain that the cellulose acetate membranes, as a whole, are too thick to yield permeability of the type normally observed, and at the same time cannot be homogenous enough to reject salt as well. Merten and co-workers (21) using electron microscopy showed existence of a thin, relatively homogenous, layer at the face of the membrane.

Kraus and Phillips (22) supplemented their study of semipermeable membranes by studying the adsorption properties of sulfides using low angle scattering techniques with respect to their structure and crystallite size and reported that very little correlation exists. Their results implied that the initial material, though largely amorphous perhaps with crystalline "centers", has amorphous regions which are relatively continuous over many hundreds of angstrom units and that during the reaction a large portion of this larger amorphous particle is transformed to a crystalline particle.

The rate and extent of conversion of these solids presumably are determined by rates of diffusion of pertinent ions in the solid. However, little is known about these diffusion rates for this type of micro-crystalline or amorphous material.

Baldwin, Holcomb and Johnson (23) in their studies of a polyacrylate-cellophane membrane found that salts having highly charged ions, either negative or positive, are rejected more strongly than salts of monovalent ions only. Also their attempt to investigate the effects of solution acidity (pH 3-11) on rejection and flow of sodium chloride has not given repoducible results; exposure to either acidic or basic media seems to affect the membrane irreversibly; however,

inorganic natural and synthetic colloids in the form of fibers and plates. These anisotropic gels with ordered particles show double refraction, swelling, and ion exchange properties. Thus it is pointed out that a definite correlation exists between organic and inorganic membranes and the existence of a common mechanism.

The formation of a crystal semi-permeable membrane from barium sulfate has been reported by Terazaua (28). He reported that the thinner the precipitated layer of barium sulfate, the less permeable the membrane.

From the above discussion, it is quite evident that it is a difficult task to make a clear-cut distinction between the theories of membrane permeability as well as to determine the behavior of the types of membranes under various conditions. Doubtless all these effects are operating to a lesser and greater degree in various membranes. This again emphasizes the essential need for more thorough knowledge of the activated fine structure of membrane material. Here again, the x-ray and electron microscopic studies of the simpler inorganic semi-permeable membranes should shed light on the fine detail structure of semi-permeable membranes, portraying the true mechanism for permeability. After this mechanism has been established, this will allow larger semi-permeable, highly efficient membranes to be constructed for the desalting of water.

Although nearly all the work on inorganic semi-permeable membranes which has been reported in literature deals chiefly with the copper ferrocyanide, semi-permeable membranes of cobalt ferrocyanide, nickel ferrocyanide, manganese ferrocyanide have been reported by Malik and Siddiqui (29) and Bhaltachanja (30).

In support of the ion exchange mechanism, Seifer (31) reported the ion exchange properties of cupric ferrocyanide and the zeolite type of gas and vapor adsorbent were attributable to the channel-like structures in the thin cubic lattice. Seifer has also used the copper ferrocyanide membrane in extraction studies, and found that the degree of extraction varies with the hydrogen ion concentration.

Karpaova, Leonava, and Logvinova (32) studied ion exchange properites of cupric ferrocyanide membranes and stated that the exchange properties depend upon the anion of the copper salt. The relationship of the cupric ferrocyanide membrane with hydrogen ion concentration act as an ion exchanger of the mixed resin type showing properties of both strong and weak acid. Also some of the studies of Freise (33) pointed out that a precipitate of cupric ferrocyanide-rich in ferrocyanide ions acts as a cation exchanger and the copper

TABLE

Condition of Drying	% Water	water adsorbed per gram of $Cu_2Fe(CN)_6$ (dry basis) Conc. of Sugar Solution, % 5	10	20	40	60
Air-dried at room temperature	31.4	-	0.245	0.201	0.200	0.140
Air dried at 80°	13.8	0.27	0.227	0.225	0.222	0.209
Dried over conc. sulfuric acid	6.9	-	0.239	-	0.180	0.147
Dried in oven at elevated temperature (assumed to be completely dry)	0.0	-	0.182	0.150	0.134	0.132

investigators assumed that all of the water present in a given gel (prepared and dried under specific conditions) comprised a definite hydrate. Some of these results are given in the following table:

Investigator	$H_2O/Cu_2Fe(CN)_6$
Wybrouboff (36)	10
Rammelsberg (37)	7
Wybrouboff (36)	6
Tinker (17)	3
Hartung (11)	3

However, Lowenstein (38) observed a continuous loss of water from cupric ferrocyanide gel dried over varying concentrations of sulfuric acid. Hartung (11) obtained a partial isotherm, employing the classical method of van Bemmelen (39) but was concerned because air in the apparatus delayed the attainment of equilibrium. The incomplete isotherms of Hartung were not sufficent to establish the existence of a definite hydrate, as he was aware. Weiser, Milligan, and Bates (40) obtained continuous isotherms for the adsorption of water on cupric ferrocyanide gels and concluded that definite hydrates were not formed. Keggin and Miles (41) considered it possible that water molecules were

channels (45) in the lattice between the relatively large ferrocyanide or ferri-cyanides ions, after the manner of certain zeolites that do not contain water molecules in definite crystallographic positions. In 1942, Weiser, Milligan and Bates (46,47) examined numerous heavy metal ferro- and ferri-cyanides, and proposed in space group $Fm3m/O_h^5$ that four Fe atoms were located in the 4(a) positions, four M_I atoms were located in the 4(b) positions, twenty-four C and twenty-four N atoms were located in the 24(e) positions, in agreement with Keggin and Miles and van Bever, but that 0 to 4 M_{II} atoms were distributed statistically in the 8(c) positions in contrast to other hypotheses. Intensity calculations for several ferrocyanides and ferricyanides gave reasonably good agreement with experiment for parameter values $X_C = 0.19$ and $x_N = 0.31$. These same parameter values were found by van Bever to be suitable for his divalent ferricyanides. The general features of the 1942 structure has been found acceptable (49,51) for numerous divalent hexacyano complexes such as $M_3[X(CN)_6]_2$, where M = Mn, Fe, Co, Ni, Zn, Cd, Cu, or Cr, and X = Co, Cr, Mn, Rh, or Ir.

E. *Electron Diffraction Studies.* In 1937, Fordham and Tyson (52) for the first time demonstrated by electron diffraction studies that cupric ferrocyanide membranes may be crystalline. They reported crystal sizes in the range of 100 to 200 Å. Fordham and Tyson concluded that any correlation between permeability and pore size as obtained by the usual microscopic methods is fortuitous. Weiser, Milligan and Bates (45) found that this pattern agreed with their x-ray diffraction patterns of the moist, undried gel and the air-dry powder, as well as with their electron diffraction patterns. From the close agreement of the x-ray patterns (for the moist gel and air-dried powder) and electron diffraction patterns obtained in a vacuum where essentially all of the water is lost (cf. *supra)*, it is not likely that the gel is a definite hydrate.

Information concerning the structure and morphology of cupric ferrocyanide gels from electron microscopic studies is very scanty or non-existent.

III. SEMI-PERMEABILITY (M. Uda and J. J. McCoy)

Several heavy metal cyanide membranes were deposited in porcelain filter crucibles (Coor's and Royal Berlin), with porous bottoms. Copper ferrocyanide membranes were made in various filters by placing a dilute solution of $K_4Fe(CN)_6$ on one side of a filter and a dilute solution of $CuSO_4$ on the other side of the filter. Some of the additional filters tried were as follows: Whatman extraction thimbles, various plastic filters, cellulose dialyzing membranes, millipore filters (0.05 μ pore size), porous clay plates and clay

ferricyanide, cobalticyanide (ACS reagent grade), or hydroferrocyanic acid, prepared as previously (53) described, employing a rapid mixing device (53). The potassium ferrocyanide and hydroferrocyanic acid solutions were always prepared not more than twenty minutes prior to the precipitation step, in order to minimize possible air oxidation and decomposition by light. Possible contamination of potassium ferrocyanide solutions by bacteria is also avoided by using only those freshly prepared solutions. The dried hydroferrocyanic acid powder exhibited a pure white color when prepared and was stored in the dark in a desiccator to prevent the formation of blue decomposition products.

The resulting gels were always precipitated with a 5% excess of the metal salt, in order to minimize potassium ion contamination, as well as to avoid excessive peptization of the precipitates, which renders washing more difficult.

The precipitation was carried out in a rapid mixing device at room temperature. The resulting suspensions of the freshly precipitated gels were washed ten times with distilled water in a centrifuge at 3000 r.p.m. and was allowed to age under water at room temperature. Aliquots of the gels were removed at varying periods of time and air-dried for x-ray diffraction examination. Upon aging, some of the diffraction patterns from the aged gels (*i.e.*, cupric ferrocyanide, cobaltous ferrocyanide, cobaltous cobalticyanide, and nickelous cobalticyanide) exhibited extra spacings corresponding to large d/n values in the range of 10 Å as well as several additional lines throughout the Debye-Scherrer diffraction pattern. The significance of the large additional spacings observed for cupric ferrocyanide has been discussed elsewhere (61). The samples of these four compounds used for the crystal structure analysis were taken prior to the appearance of such additional spacings.

In general, the samples were allowed to age for several weeks in the hope of growing larger crystals which would give sharper diffraction lines. However, little or not detectable change occurred after a period of six weeks, at which time the gels were suction-filtered using Whatman #42 filter paper and then allowed to air-dry.

b. Dehydration Isobars. In order to establish the dehydration behavior of the 30 compounds considered in this report, careful dehydration isobars were obtained in an apparatus already described (11, 17, 37, 72, 74). The samples were heated to constant weight in a thermostatically controlled electric oven, in a current of air containing water vapor at a constant partial pressure of 17.54 mm of Hg (corresponding to 20°C.). The temperature of the oven was controlled to better than 0.5°C. and at least two weeks were required to attain equilibrium at each temperature point (2°C. intervals) on the

		(0,0,0; 0,1/2,1/2; 1/2,0,1/2; 1/2,1/2,0) +
4 Fe	(4a)	0,0,0;
4 M_I	(4b)	1/2,1/2,1/2,
0-4 M_{II}	Statistically in (8c)	1/4,1/4,1/4; 3/4,3/4,3/4;
24 C	(24e)	x,0,0; 0,x,0; 0,0,x; $\bar{x}$,0,0;0,$\bar{x}$,0; 0,0,$\bar{x}$.
24 N	(24e)	

The sequence -Fe-C-N is assumed, rather than -Fe-N-C, on the basis of (a) the elegant neutron diffraction results of Curry and Runciman (58) for potassium cobalticyanide, and Sequeira and Chidambaram (59) for potassium zinc cyanide, and (b) the discussion of Shriver, Shriver, and Anderson (60). In view of the similarity of f_j for C and N, it is difficult to make a clear distinction between these two possible sequences from x-ray intensity calculations. The parameter values were refined by full least squares treatment, starting with the two position parameters suggested earlier (46), five isotropic temperature factors, and a scale factor. Because of limited storage capacity available to us, the calculations, made with an IBM-1620 Computer were divided into several programs. The refinement was continued for at least six cycles.

The final values of $R = \Sigma||F_o| - |F_c|| / \Sigma|F_o|$, the two positions parameters, and five isotropic temperature factors are given in Table I, together with the corresponding Fe-C, Co-C, C-N, and N-M distances.

2. RESULTS AND CONCLUSIONS.

a. Dehydration Isobars. The thirty dehydration isobars given in Fig. 1 are based on closely agreeing duplicate determinations, made at temperature intervals of 2°C. from 30° to 60°C. The numerous experimental points fall exactly on the curves as drawn. The individual points are omitted for the sake of clarity. It will be noted that all of the dehydration curves are bivarient, with no indication of inflection points or discontinuities that would indicate the presence of combined water. The x-ray diffraction pattern does not change in any detectable way, during the loss of water, during the course of the dehydration isobar in the temperature range 30-60°C. An isobar not reproduced for *longer aged* cupric ferrocyanide containing sheet-like particles and exhibiting extra diffraction lines, shows a definite step corresponding to eight moles of water per mole of $Cu_2Fe(CN)_6$, and has been discussed elsewhere (61).

The isobaric experiment was continued at temperatures well above 60°C. to around 100-130°C. After the horizontal flat region of

the isobars, extending to about 60°C. and corresponding to the anhydrous sample, additional loss of weight occurs at higher temperatures depending on the particular sample. This additional loss of weight corresponds to decomposition of the sample, and has been verified by x-ray diffraction analysis. As the various compounds begin to decompose, the x-ray pattern corresponding to the complex cyanide disappears. For example, when cupric ferrocyanide is heated in air to 300°C., the x-ray diffraction pattern corresponds to a mixture of cupric oxide and ferric oxide (α-Fe_2O_3). Furthermore, Cyanogen-containing gases are evolved from the samples at temperatures in the range of 65-130°C. In separate experiments, several complex cyanides, including cupric and cadmium ferro-, ferri-, and cobalti-cyanides, were heated to about 200°C., and liquid cyanogen was collected in a liquid nitrogen trap, some formation of the black polymer (62) being observed as the liquid cyanogen warmed on removal of the cold trap.

It is believed that the results of the isobaric dehydration are sufficiently conclusive to allow one to assume that the water content of the air-dried samples corresponds to adsorbed water and/or zeolitic water (cf. 40, 45, 48-51), and that one does not need to place water molecules in definite crystallographic positions in the unit cell.

b. Lattice Constants and Densities. X-ray Debye-Scherrer patterns for thirty complex cyanides are shown in Figs. 2-7. Observed and calculated interplanar spacings, observed intensities, observed and calculated F values and F values are listed in M. L. Beasley's thesis (66). The lattice constants for 30 complex cyanides are summarized in Table I. These are based on the average of several microphotometer tracings of several separate photographs employing Fe K x-radiation (manganese beta filter). The values listed are based on (a) agreeing calibrations using silicon and sodium chloride standards and (b) Cohen's difference method (63) of least squares. Similar calculations based on diffractometer tracings agree to within the standard deviation listed in the table. The lattice constants are in reasonably good agreement with some uncorrected values given in the literature (48-51). The lattice constants will be discussed from another viewpoint below (Part IV).

The following values of a_o for cupric ferrocyanide have been reported (all based on uncorrected d/n values): Rigamonti (42) 9.98 ± 0.05 Å; Fordham and Tyson (52) 9.956 Å; Weiser, Milligan, and Bates (46) 10.02 Å; Hanawalt, Rinn, and Frevel (78) 10.00 Å. In Table II there is given observed and calculated interplanar spacings for a cupric ferrocyanide sample aged 6 hours.

The observed and calculated densities for the thirty

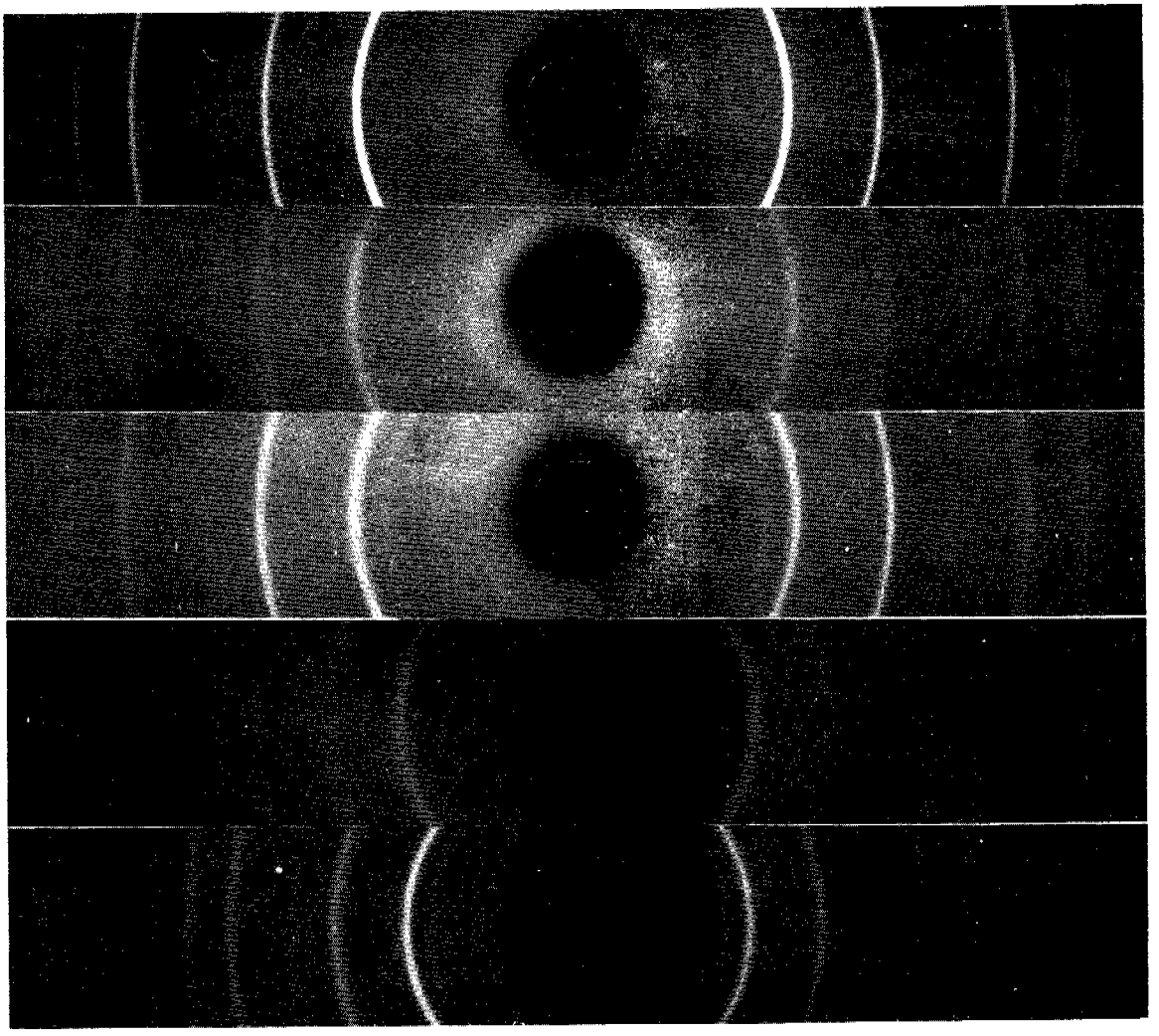

Fig. 3. X-ray diffraction patterns for the following cubic crystals; A, nickel ferrocyanide (Fe Kα radiation); B, palladium ferrocyanide (Fe Kα radiation); C, cobaltous ferrocyanide (Fe Kα radiation); D, gallium ferrocyanide (Cu Kα radiation); E, indium ferrocyanide (Cu Kα radiation).

compounds are likewise listed in Table I. All of the observed values are a few percent lower than the calculated values. In view of the difficulties involved in experimental densities for finely-divided powders, we believe that the close agreement reported here results in part from a partial cancellation of errors, where voids tend to give low results, and adsorbed material such as water tends to give a high result.

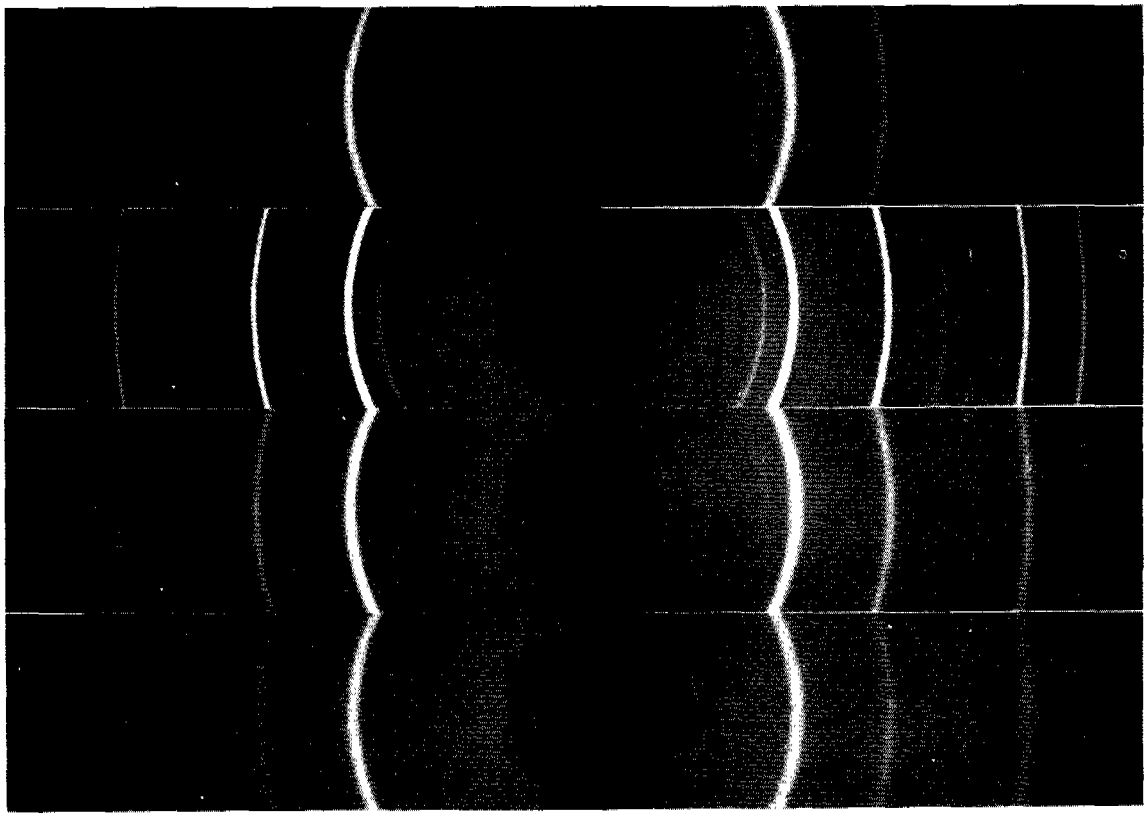

Fig. 5. X-ray diffraction patterns (Fe Kα radiation) for the following cubic crystals: A, nickel ferricyanide; B, cupric ferricyanide C, ferrous ferricyanide; D, titanium ferricyanide.

the standard deviation (Computation B, Tables, III and IV). The final values of the parameters and temperature factors for $Cu_2Fe(CN)_6$ are listed in Table IV, and Table V, together with some interatomic distances.

The basic differences in the parameters obtained from Computation A and Computation B is that minimum observable F values and superimposed reflections having the same d/n values (example [333-511]) were considered in Computation A but were omitted in Computation B.

Ferrari, Tani, and Magnano(50) suggested the possibility that in certain isomorphous divalent metal cobalticyanides the space group may be F43m, where two M_{II} atoms are statistically distributed in the 4c positions rather than in the 8c positions of Fm3m. These investigators did not employ absorption or temperature factors, and obtained for $Cd_3[Co(CN)_6]_2$ a Co-C distance of 2.05 Å, a C≡N distance

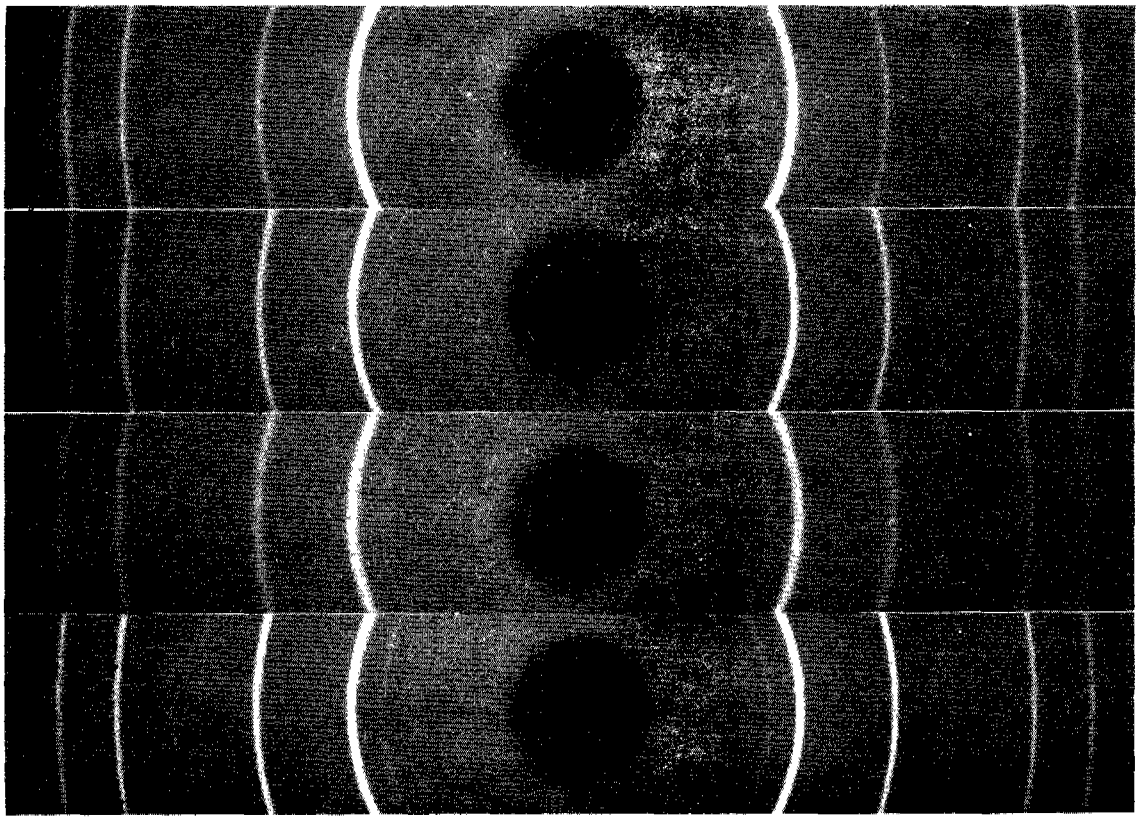

Fig. 7. X-ray diffraction patterns (Fe Kα radiation) for the following cubic crystals: A, titanium cobalticyanide; B, cobaltous cobalticyanide; C, nickel cobalticyanide; D, cupric cobalticyanide.

are larger for $Cu_2Fe(CN)_6$ than for $Cd_3[Co(CN)_6]_2$ because in the former there are 4 Cu_{II} atoms to distribute statistically, whereas, in the latter there are only 2 Cd_{II} atoms to distribute statistically. We have found for cupric ferrocyanide that a very large R value of 0.19 is obtained if the parameters in Table III are used in space group $F\bar{4}3m$. Furthermore, complete parameter refinement starting with these parameters leads, in $F\bar{4}3m$, to a R value of 0.11 (almost double the R value from the Fm3m space group) and with a Fe-C distance of 1.33 Å, and C≡N distance of 0.69 Å. This Fe-C distance is much too small, as it is approximately the value of the covalent radius of Fe(II). This C≡N distance also is much too small as it corresponds approximately to the the covalent radius of carbon alone. It is concluded that the structure cannot be considered to be based on $F\bar{4}3m$.

TABLE II

OBSERVED AND CALCULATED INTERPLANAR SPACINGS FOR $Cu_2Fe(CN)_6$

$a_o = 10.013 \pm 0.001$ Å.

hkl	d/n obs.	d/n calc.
111	5.7818	5.7810
200	5.0042	5.0065
220	3.5400	3.5401
311	3.0196	3.0190
222	2.8905	2.8905
400	2.5032	2.5033
420	2.2390	2.2390
422	2.0440	2.0439
333 511	1.9269	1.9270
440	1.7700	1.7701
531	1.6926	1.6925
442 600	1.6685	1.6688
620	1.5830	1.5832
622	1.5100	1.5095
444	1.4452	1.4453
640	1.3880	1.3886
642	1.3380	1.3380
800	1.2515	1.2516

d. Interatomic Distances. The observed value of 1.872 ± 0.004 Å for the Fe-C distance agrees closely with the following: Co-C = 1.89 Å in $K_3Co(CN)_6$ (Curry and Runciman, 58); Fe-C = 1.89 Å in $H_4Fe(CN)_6$ (Pierrot, Kern, and Weiss, 1966). The observed value of 1.143 ± 0.003 Å for C≡N distance is in good agreement with the following: 1.15 Å in $K_3Co(CN)_6$ (Curry and Runciman, 58); 1.15 Å in $H_4Fe(CN)_6$ (Pierrot, Kern, and Weiss, 64); 1.157 ± 0.009 Å in $K_2Zn(CN)_4$ (Sequeira and Chidambaram, 59); 1.150 to 1.157 Å in several cyanides (Pauling, 65).

If it is assumed that the nitrogen has a covalent radius of 0.547 Å (Pauling, 65) in this compound, then the "radius" of the ferrocyanide ion is 3.58 Å, which may be compared with an estimate of 3.6 Å made by one of us (46). If anion contact is assumed, the "radius" of the ferrocyanide ion is 3.54 Å.

TABLE IV

$Cu_2Fe(CN)_6$; $a_o = 10.013 \pm 0.001$ Å

	Computation A	Computation B -Fe-C-N-		Computation B -Fe-N-C-		
Position Parameters						
x(C)	0.1883	0.1871	± 0.0004	0.1825	± 0.0035	X(N)
x (N)	0.3029	0.3006	± 0.0003	0.2917	± 0.0044	X(C)
Interatomic Distances, Å						
Fe-C	1.885	1.872	± 0.004	1.827	± 0.036	Fe-N
C N	1.148	1.143	± 0.003	1.093	± 0.041	C N
$N-M_I$	1.974	1.991	± 0.004	2.041	± 0.041	$C-M_I$
Temperature Factors, Å^2						
B(fe) *(4a)*	1.26	1.40	± 0.49	0.80	± 0.53	B(fe)
B(C) *(24e)*	2.49	4.35	± 2.17	7.69	± 1.78	B(N)
B(N) *(24e)*	2.55	1.87	± 1.35	-1.46	± 1.21	B(C)
$B(M_I)$ *(4b)*	1.36	0.88	± 0.37	1.60	± 0.44	$B(M_I)$
$B(M_{II})$ *(8c statistically)*	2.86	3.14	± 0.44	3.42	± 0.52	$B(M_{II})$
R value	0.059	0.055		0.075		

In view of the relatively small number of Debye-Scherrer lines observed for cupric ferrocyanide and the eight parameters employed in the least squares refinement, it is difficult to make a reliable estimate of the possible errors in the distances and temperature factors. Indeed, we consider that a *single result*, such as for cupric ferrocyanide, may be of little significance by itself. However, we have carried out quantitative studies (Beasley and Milligan, submitted for publication) on a series of 30 isomorphous compounds involving ferrocyanides (Cd^{+2}, Tl^{+3}, Sc^{+3}, Mn^{+2}, Fe^{+2}, Ti^{+3}, In^{+3}, Ni^{+2}, Pd^{+2}, Ga^{+3}, Co^{+2}, Al^{+3}, and Be^{+2}), ferricyanides (Cd^{+2}, Tl^{+3}, In^{+3}, Mn^{+2}, Co^{+2}, Ni^{+2}, Cu^{+2}) and cobalticyanides (Cd^{+2}, Tl^{+3}, In^{+3}, Mn^{+2}, Fe^{+2}, Ti^{+3}, Co^{+2}, Ni^{+2}, Cu^{+2}). Refinement of the data for these

B. Hexagonal Heavy Metal Ferro- Ferricyanides. [Wayne E. Bailey]

Weiser, Milligan and Bates (46) observed that heavy metal ferrocyanides and ferricyanides were cubic (Fm3m) if the metal cation "radius" was less than that for cadmium. For example, lanthanum, and neodymium ferrocyanides exhibited an isomorphous structure more complicated than cubic. Lanthanum ferricyanide also was not cubic, and its x-ray diffraction was similar but not identical with the above mentioned ferrocyanides. Furthermore, cadium and zinc ferrocyanides have exhibited both a cubic and a non-cubic form when made under various conditions of precipitation. The exact conditions under which the two forms may be prepared are not known.

Beasley (66) confirmed the existence of the non-cubic forms and demonstrated that yttrium ferrocyanide also could be made in a non-cubic form isomorphous with the corresponding neodymium and lanthanum compounds.

Several ferrocyanides and ferricyanides of large trivalent cations have been prepared. Among those thus far studied are the ferrocyanides of ytterbium, neodymium, praseodymium, lanthanum, and bismuth, listed in increasing "radius" of the cation. Of special interest is the bismuth compound, since bismuth (r^{3+} = 1.20 Å) is the largest trivalent metal ion available. All of these ferrocyanides form a non-cubic isomorphous series, and the results agree closely with the work of Weiser, Milligan and Bates (46). Reproductions of some of these x-ray diffraction patterns are given in Figure 8. It will be noted that all of the patterns are very similar, and that only a slight shift in the lattice constants is involved, suggesting that, as in the cubic isomorphous series, the large ferrocyanide ion packing is controlling the size of the unit cell. The spacings have been approximately indexed in the hexagonal system, employing only the strongest lines. Because of the small size of the crystals thus far made, doubt exists concerning some very weak lines. The exact indexing will be continued from x-ray photographs made from samples exhibiting larger crystals, and hence sharper lines.

There is a distinct possibility of preparing larger crystals of the corresponding ferricyanides, especially those of lanthanum and bismuth. For example, lanthanum ferricyanide is said to be fairly soluble in water, as compared with other similar compounds. Indeed, lanthanum ferricyanide solutions have been studied as examples of a salt solution with both trivalent cations and anions.

In a few preliminary experiments lanthanum and bismuth ferricyanides have been prepared, and substantially much sharper and

In continuation of the work with trivalent metal ion ferrocyanides, ytterbium, yttrium, neodymium, praseodymium, lanthanum, and bismuth ferricyanides have now been prepared in this laboratory. These ferricyanides exhibit x-ray patterns isomorphous with those shown by the ferrocyanides, differing only slightly, due to small changes in the lattice constants and adsorption factors for each compound. The reproduction of the x-ray diffraction patterns given in Figure 9 compare the ferrocyanide pattern (bismuth) to some typical ferricyanide patterns (bismuth, neodymium, praseodymium, and lanthanum.)

It is of interest that the ferrocyanides of metal with a valence of four have the same ratio of metal ion to cyanide ions as the tri-valent ferricyanide, $M^{+4}[Fe(CN)_6]^{-4}$, thus suggesting that some of these ferrocyanides may belong to this isomorphous series. As expected, the ferrocyanide prepared from thorium (four valance) exhibited an x-ray pattern similar to the trivalent ferri- and ferrocyanides. Thus any variations in intensities of the x-ray diffraction lines between the compounds of bismuth ferricyanide and thorium ferrocyanide due to the difference of the scattering power of the bismuth and thorium ions, may become an important factor in determining the positions of the metal ions in calculations involving the structure determination.

Large single crystals of neodymium, praseodymium and lanthanum ferricyanides, suitable for x-ray analysis using the Buerger precission and Weissenberg cameras, have been prepared and tentative values for the lattice constants have been obtained. These values are now being refined with the aid of their respective powder patterns. The single crystal of lanthanum ferricyanide was prepared as follows: (The preparation of all crystalline samples was similar). Lanthanum Oxide (99.99%; ACS grade) was dissolved in the stoichiometric quantity of dilute hydrochloric acid, and the solution was cooled and diluted to give a concentration of 0.2 grams to 5 ml of solution. The calculated volume of saturated potassium ferricyanide (giving a 10% excess of the La^{3+} ion) was added and the solution was allowed to stand in the dark. Crystallization was usually complete in two days to three days.

The composition of the crystals has been determined to be as shown in Table VI.

	Sample I	Sample II
Carbon	16.59%	16.57%
Hydrogen	2.29%	2.24%
Nitrogen	19.10%	19.71%
Iron	12.88%	12.71%
Chlorine	0.00%	0.00%
Potassium	0.00%	0.00%

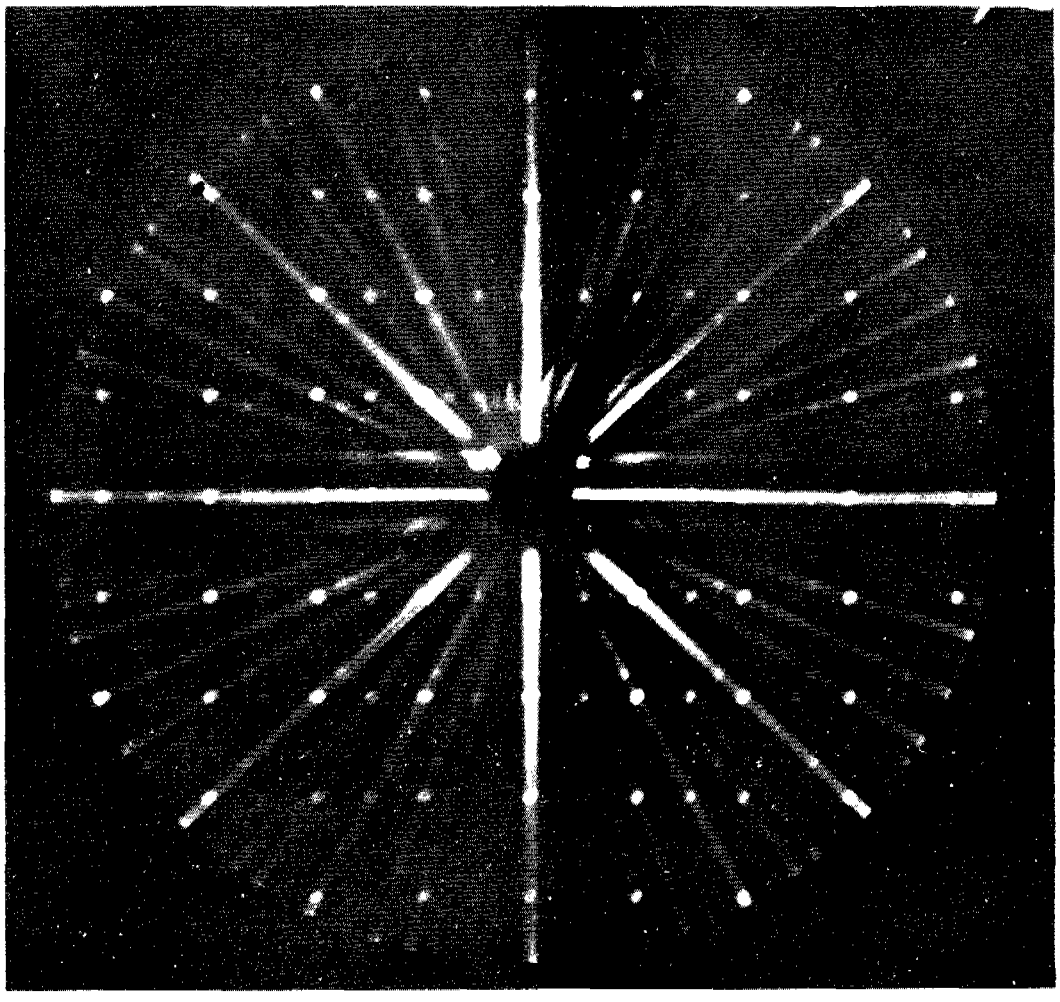

Fig. 10. X-ray diffraction precession camera photograph (Ag K radiation) for hexagonal lanthanum ferricyanide.

Shown in Fig. 10 is the (hhl) lattice net of lanthanum ferricyanide obtained, using silver K radiation, with the precession camera (no filter, $\mu = 20^{\circ}$). Fig. 11 shows the reproduction of a typical Weissenberg photograph from a Lanthanum ferricyanide crystal, mounted with c-axis parrellel to the dial axis. The zero level of the hk0 reflections gives the a_o distance and proves that the crystal is definitely hexagonal. Photographs have been taken using each of the three types of single crystals and each has been shown to be hexagonal. Work of the evaluation of the intensities is proceeding in order to evaluate the structures.

ducer plate of a 3 megahertz ultrasonic device. The resulting mist was allowed to settle on a carbon membrane for electron microscopy and electron diffraction examination. The small droplets of the suspension which comprise the mist are about 5 microns in diameter and dry on the carbon membrane within a few seconds. Thus it is possible to produce an air-dry sample of the cupric ferrocyanide gel that has not aged more than 15 to 20 seconds after precipitation. It is assumed that the aging phenomenon under study does not occur at a detectable rate in air-dry samples, *i.e.*, the aging takes place only when the gel particles are in contact with the liquid water.

Series B. The cupric ferrocyanide gels designated here as *Series B* were prepared from 0.01 N solutions of cupric sulfate and potassium ferrocyanide as described under *Series A*. The freshly precipitated gel was washed ten times with distilled water in a centrifuge at 3000 r.p.m. and allowed to age under water at room temperature. Aliquots of the gel were removed at varying periods of time and air-dried for electron microscope, electron diffraction, and x-ray diffraction examination.

Series C. The cupric ferrocyanide gels designated here as *Series C* were prepared as described under *Series B*, except the temperature of precipitation was 99-100°C., and the gel was washed ten times in a centrifuge at 3000 r.p.m. with distilled water at 80°C. The washed gels were aged under water at 100°C., employing a reflux condensor. Aliquots were removed and air-dried on carbon membranes at varying periods of time for electron microscopic examination.

Series D. Samples of cupric ferrocyanide gels designated herein a *Series D* were prepared as described above using 0.01 N solutions of cupric sulfate and hydroferrocyanic acid at room temperature, followed by washing ten times in a centrifuge at 3000 r.p.m. the washed gels were aged for several months after varying periods of time, and were air-dried for electron microscopic examination.

b. Electron Microscopy. All electron microscopic and electron diffraction studies were carried out with a Seimens "Elmiskop I" (1960 model but updated in 1965) at 100 kV, with a magnification on the negatives of 40,000, 80,000 or 160,000 diameters.

Carbon membranes were prepared in a Seimens vacuum evaporator by deposition of carbon on freshly cleaved "television" grade mica. The carbon membranes were transferred under water to 400 mesh Athene copper grids.

Samples of cupric ferrocyanide were placed on the carbon membranes by producing a mist of the aqueous suspension in a 3

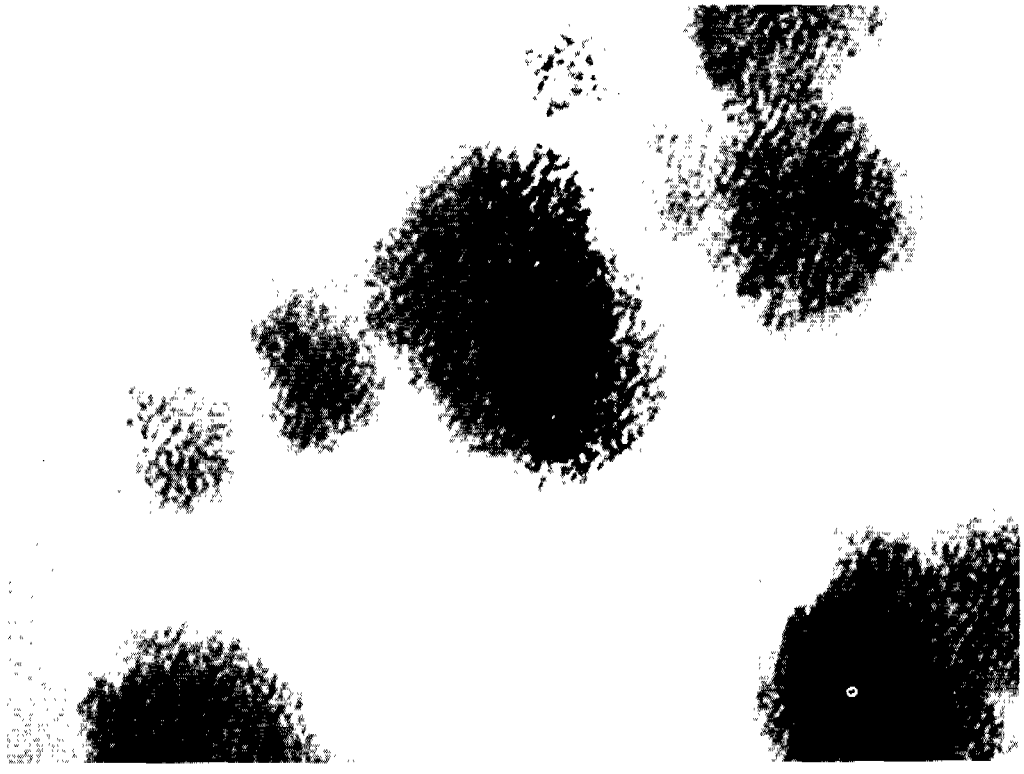

Fig. 12. Electron micrograph of cupric ferrocyanide gel precipitated and washed on carbon membrane. Mag. 320,000 diameters [after Kanesaka (76)].

particles are slightly larger, and they are grouped into slightly closer packed aggregates. Fig. 13C (upper) refers to ten minutes of aging, and the primary particles have definitely increased in size; much larger aggregates are present, as was observed for aging alumina (75). Fig. 13D (upper) corresponds to fifteen minutes of aging. Here particles as large as 30 to 40 Å have appeared, and a suggestion of sheet-like aggregates is becoming visible, as was also observed for aging alumina (75). In the corresponding electron diffraction patterns in Fig. 13A to 13D (lower) it will be noted that the 20-second sample is amorphous in the sense that the pattern is like that from a liquid, and that the crystallinity increases with time of aging, until the 15-minute sample corresponds to definitely crystalline cupric ferrocyanide. It will be further noted that the amorphous bands become fainter as the crystalline lines appear, indicating a transformation of the amorphous material into crystalline material, rather than the growth of minute "crystallites" (perhaps considered too small to yield definite diffraction bands) to larger and larger crystals. However,

after formation, the small crystals increase in size (as depicted by the diffraction lines becoming sharper) as the aging proceeds. This behavior is in partial contrast to that of the aging of freshly precipitated $Nd(OH)_3$ where the amorphous neodymia (53) ages to produce crystals, the diffraction lines of which increase in amplitude, while maintaining an approximately constant width as the aging proceeds.

b. Aging Under Water at Room Temperature. The twelve electron micrographs in Figs. 14 and 15 (A to L) correspond to well-washed cupric ferrocyanide gels (*Series B*) aged for periods of time from 20 seconds to six months. It will be noted that as the aging proceeds, the minute 10 Å primary particles increase in size, and that they pack into more dense aggregates; finally after 10 to 24 hours sheet-like particles appear. After 24 to 48 hours, some of the particles show sharp crystal edges, and the formation of sheets becomes very evident.

The aging phenomena is also illustrated by the composited electron diffraction patterns shown in Fig. 16, where A refers to 6 hours of aging and B refers to 24 hours. These two patterns correspond to the normal pattern of cupric ferrocyanide. However, in Fig. 16C there will be noted the appearance of two additional lines of larger interplanar spacings (10.0 Å and 7.1 Å). Three extra lines are clearly visible in Fig. 16D, corresponding to spacings of approximately 10.0 Å, 7.1 Å, and 4.48 Å. The electron diffraction patterns of Fig. 16C and 16D arise from a sample area consisting predominately of sheet-like material. The possible significance of these extra diffraction lines will be discussed below.

In the samples aged long enough to produce plate-like sheet material, there are occasionally observed rolls or scrolls as illustrated in Figs. 17A and 17B. These rod-like particles depicted at 160,000 diameters are similar to those already reported for halloysite clay (77), alumina (75) and neodymium trihydroxide (53) and will not be discussed further here.

c. Aging Under Water at 100°C. Aging of cupric ferrocyanide proceeds about six times faster at 100°C. than at room temperature as shown in Fig. 18. It will be noted that sharp crystal edges are evident after only an hour of aging, and substantial amounts of plate-like sheets exhibiting the additional large spacings, appear in about six hours.

d. Water Content of Cupric Ferrocyanide. Preliminary experiments indicated a difference in the water content of cupric ferrocyanide samples (a) aged sufficiently to yield sheets or plates, as evidenced by their appearance in electron micrographs, and (b)

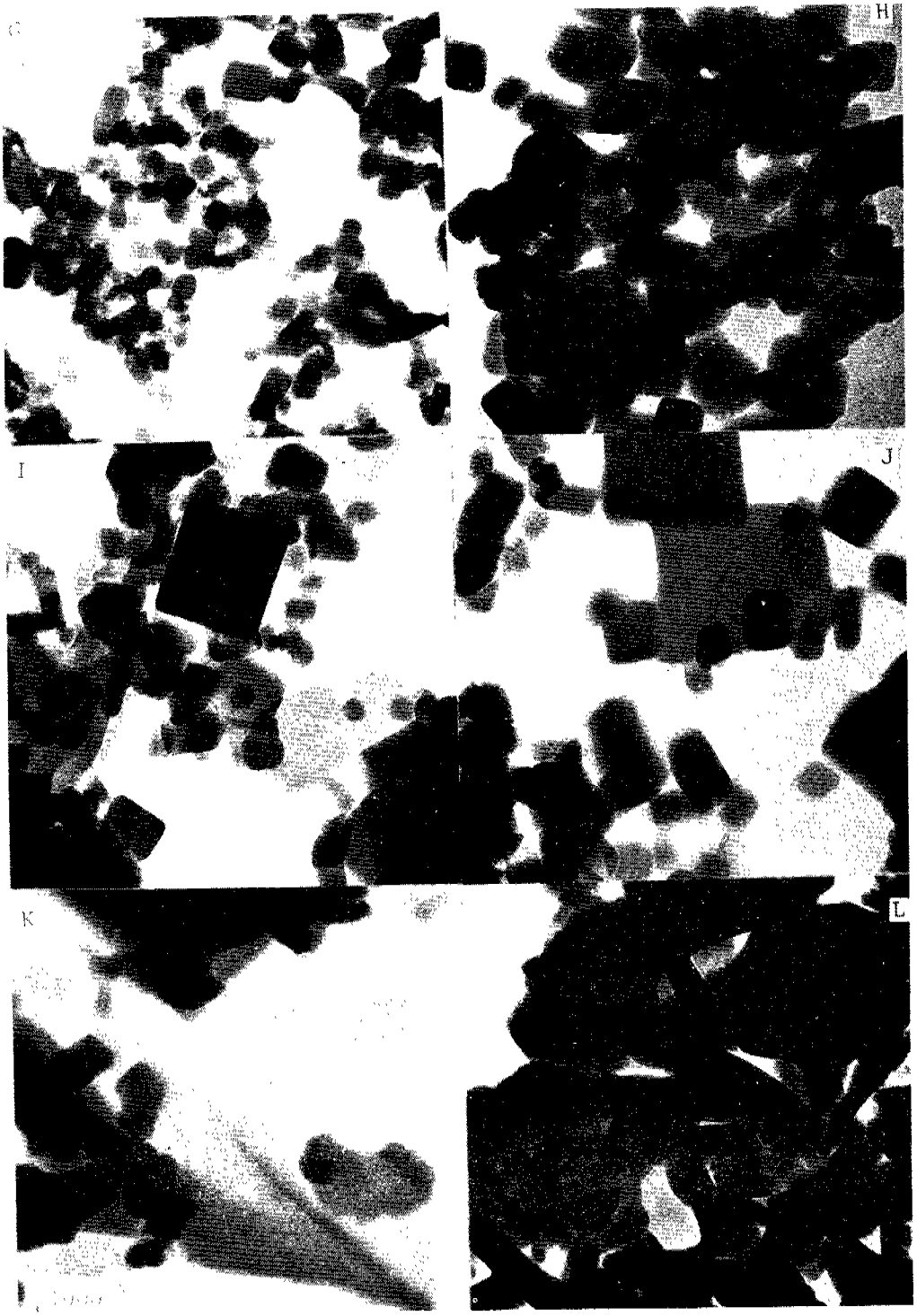

Fig. 15. Electron micrographs of washed cupric ferrocyanide aged under distilled water at room temperature for: G, 36 hours; H, 48 hours; I, 60 hours; J, 6 days; K 6 weeks; L, 6 months.

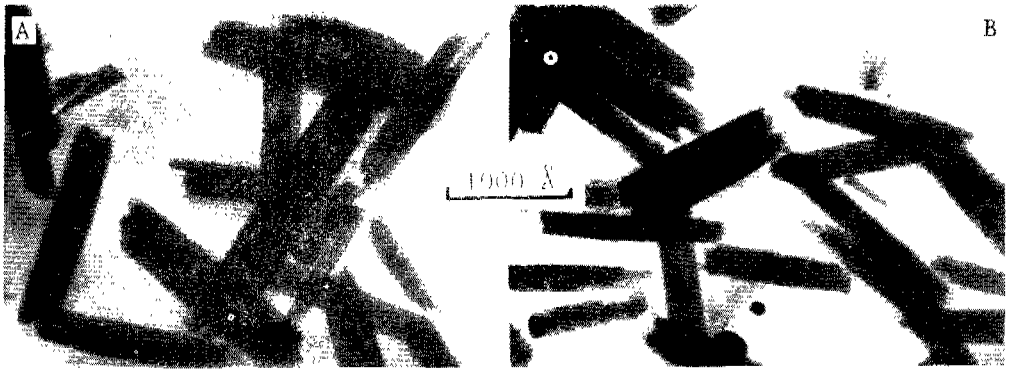

Fig. 17. Electron micrographs of aged cupric ferrocyanide exhibiting rolled sheets or scrolls.

microscope for a period of 48 hours, and then it yielded the electron diffraction pattern shown in Fig. 19B, which corresponds exactly with the normal pattern of unaged cupric ferrocyanide. This result suggested that the loss of the extra diffraction lines could be associated with the loss of water. This hypothesis was verified by exposing the sample, still mounted on its carbon membrane, to moist laboratory air for about 30 minutes, after which it yielded the diffraction pattern shown in Fig. 19C, which is identical in all respects to the oribinal pattern (Fig. 19A). This cycle of operations may then be repeated as often as desired. In Fig. 19C, the extra lines attributed to the presence of added water are indicated at 1, 2, and 4, whereas the lines marked 3 and 5 correspond to the normal unaged cupric ferrocyanide pattern.

f. Dehydration-Rehydration Isobars. In order to further verify the hypothesis that the above mentioned extra diffraction lines are associated with water content differences, dehydration-rehydration isobars were obtained for the aged cupric ferrocuanide sample of Fig. 19A. In Fig. 20, Curve A (open circles) corresponds to a dehydration isobar (H$_2$O 17.54 mm. of Hg) and Curve A (closed circles) corresponds to a rehydration isobar at the same partial pressure of water vapor. It will be noted that the dehydration and rehydration isobars may be represented by the same curve, indicating that the equilibrium values may be readily reached from either direction. The isobar (curve A) corresponds to a loss of 8 molecules of water per mole of $Cu_2Fe(CN)_6$at about 49°C. The bivarient loss of water from 25° to 45°C. is attributed to the continuous loss of "zeolitic" or surface adsorbed water. Any material in finely divided form, and thus possessing a high surface area, would be expected to adsorb considerable

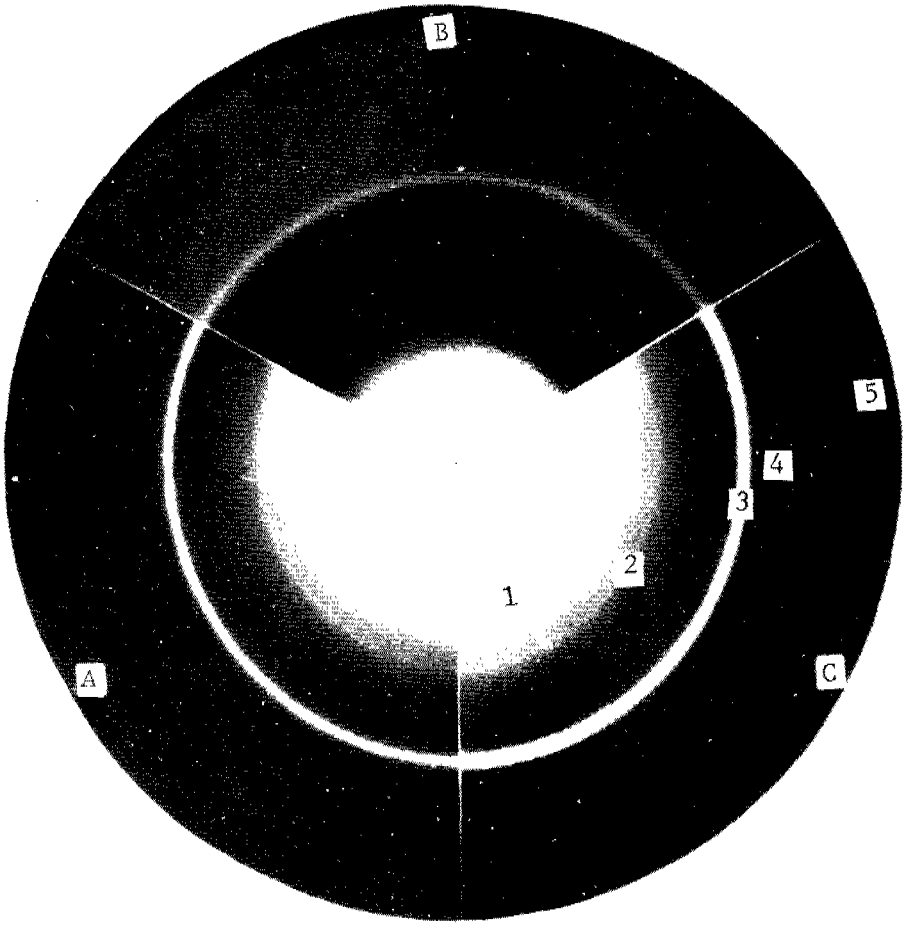

Fig. 19. Low angle electron diffraction patterns of cupric ferrocyanide: A, aged, reddish-brown sample exhibiting plate-like particles (*cf.* Fig. 18F); B, same after vacuum dehydration; C, same after rehydration in moist air.

amounts of water regardless as to whether the substance was or was not a hydrate. The bivarient region from about 50° to 56° is likewise attributed to a continuous loss of water adsorbed on the "anhydrous $Cu_2Fe(CN)_6$, produced by the dehydration of the original hydrate, $Cu_2Fe(CN)_6 \cdot 8H_2O$. The original aged sample of sheet-like material may

be formulated as $Cu_2Fe(CN)_6 \cdot H_2O \cdot xH_2O$, where x refers to the adsorbed water content. It is not intended that this formulation implies any assumption as to the structural location or state of the water.

g. X-Ray Diffraction. The phase change described in the paragraph just above was verified by x-ray diffraction patterns of samples removed* at various equilibrium temperatures during the course of the isobar of Curve A in Fig. 20. These are given in Fig. 21 where A refers to the equilibrium point at 45°C. This x-ray pattern is in agreement with the electron diffraction pattern of the plate-like $Cu_2Fe(CN)_6 \cdot 8H_2O$. It will be noted that the phase change shown in Fig. 20, based on x-ray diffraction patterns, agrees with the phase change in Fig. 19, based on the isobar.

h. Cupric Ferrocyanide Free of Sheet-like Morphology. In Fig. 20, Curve B refers to a dehydration isobar for a sample of precipitated cupric ferrocyanide that has been aged for about one hour (*vide* Fig. 14B) and contains no plate-like material detectable by electron microscopic methods, or no extra diffraction lines. This isobar represents a continuous loss of water, and does not suggest the presence of any definite hydrate. In Fig. 22, there is given x-ray diffraction patterns taken at three equilibrium points, showing that no phase change occurs during the course of this isobar (Curve B). Curve C in Fig. 20 is for a sample aged under water for about 12-18 hours (*vide* Figs. 14D and 14E), and which contains only a very small amount of sheets. It will be noted that Curve C exhibits a slight inflection point. It is deduced that this inflection point demonstrates the presence of a small amount, perhaps 5 to 8 per cent of $Cu_2Fe(CN)_6 \cdot 8H_2O$ in this sample. In this connection it will be recalled that the 1942 isotherm of Weiser, Milligan, and Bates (46) showed a very slight inflection point. Although these investigators concluded that no hydrates were formed, we are now of the opinion that their sample, likewise included a small amount of $Cu_2Fe(CN)_6 \cdot 8H_2O$. The 1942 sample was prepared by careful washing of the freshly formed gel, followed by drying in air. This procedure required around 12 to 24 hours, inasmuch as air-drying is slow. Furthermore, in the 1942 paper (46), Fig. 1 shows some weak x-ray diffraction lines, which are now known to correspond to the pattern of $Cu_2Fe(CN)_6 \cdot 8H_2O$. At least

*Because of the ease of rehydration in moist air at room temperature the samples were removed rapidly and placed in mark tubes pre-heated to the temperature of the sample. The capillary tubes were wealed as rapidly as possible in order to avoid changes in water content which would prevent the x-ray diffraction pattern from corresponding to the sample at its equilibrium point.

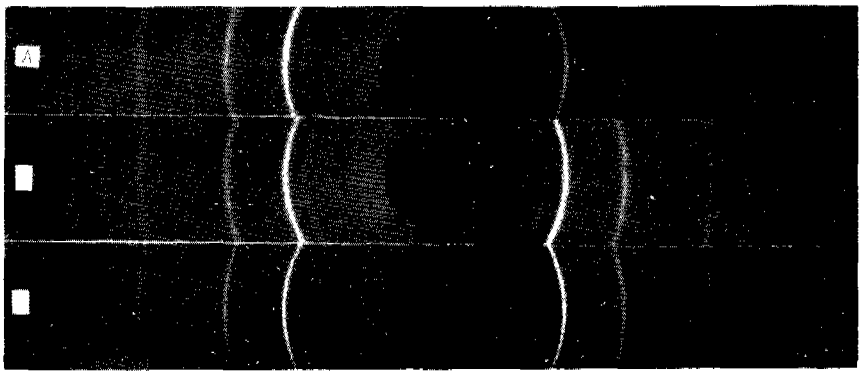

Fig. 22. X-ray diffraction patterns (fe Kα radiation) for cupric ferrocyanide (Curbe B, Fig. 20) during the course of the dehydration isobar, at the following temperatures: A, 50°C; B, 55°C.; C, 60°C.

phase, considered to be $Cu_2Fe(CN)_6 \cdot 8H_2O$, numerous attempts were made to secure single crystal electron diffraction patterns. All preliminary attenpts were completely unsuccessful. Although some of the sheets are at least 1000 x 1000 Å or more in cross-section, the single sheets are too thin to yield single crystal patterns, as was previously found for certain thin alumina sheets (75). Some success came from depositing sequentially as many as 15 separate layers, employing extremely dilute suspensions of the aged sample and the ultrasonic mist device at 3 megahertz, each layer being dried in the air prior to the deposition of the next layer. This procedure was based on the possibility that several sheets might superimpose in the proper orientation so as to make possible a good single crystal pattern. Occassionally, we were able to secure single crystal patterns, but they usually contained multiple spots, indicating two or more superimposed single crystal areas. However, the best cross-grating pattern obtained gave the normal hexagonal array of spots, characteristic of a cubic crystal oriented with the (111) faces parallel with the membrane, as is well-known in the instance of colloidal gold "trigons" (79).

In another area, a poorly developed cubic cross-grating pattern was observed for a single crystal area in a different orientation. It will be recalled that Rigamonti (42) stated that some of his 1938 electron diffraction patterns suggested orientation. We deduce that his sample, giving rise to the orientation effect, had been aged long enough to produce at least some of the sheet material.

In view of the fact that the sheets are generally oriented on carbon membranes, samples were prepared for x-ray diffraction

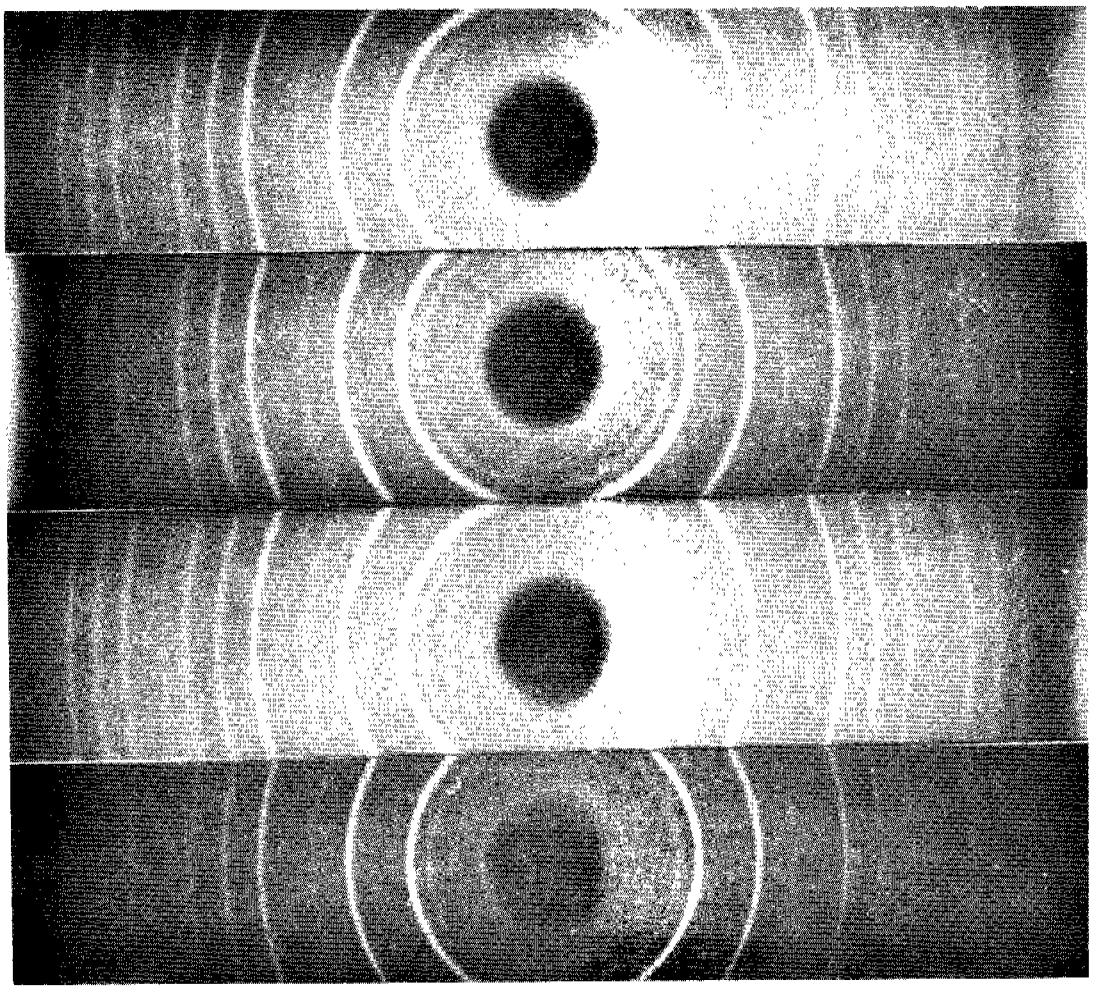

Fig. 23. X-ray diffraction patterns (Cu Kα radiation) illustrating aging effects in cupric ferrocyanide for samples aged: A, 1 month in pure water; B, 5 months in pure water; C, 10 days in hydrochloric acid (pH = 1.3); D, 1 month in hydrochloric acid (pH = 1.3).

crystallize poorly when precipitated by mixing solutions of potassium ferrocyanide and a ferric salt. However, when it is prepared in 1 M HCl, a well-crystallized Prussian blue sample results with a small amount of impurity present, and no super-structure reflections were observed.

k. Evacuation Effects. [M. Uda]. Aside from some early observations of Katz (81) in 1922 and McMahon, Hartung and Walbran

observations of Katz are fully confirmed. We have also observed that the addition of methyl alcohol, ethyl alcohol, acetone, and certain other water-miscible drying agents will change the color of reddish-brown cupric ferrocyanide gel to a blue color. Dilution of the drying solvent with additional water will reverse this color change.

The observed color change is not unique for cupric ferrocyanide. Thus Ferrani, Tani and Magnano (48) observed that rose-colored cobaltous cobalticyanide becomes "copper-blue" when dehydrated.

Evacuation effects have been observed using x-ray diffraction. Two kinds of copper ferrocyanides with and without superstructure reflections, cobaltous cobalticyanide and cadmium ferricyanide, have been studied. The copper ferrocyanide with superstructure reflections was precipitated, washed, and aged in HCl for 7 days; all other cyanides were freshly precipitated. A small amount of the powder was mounted in 0.5 mm. diameter Mark tube and evacuated using a fore pump for 1.5 hours at room temperature. The capillary tubes were then sealed and x-rayed with the sample in a vacuum. Figs. 24 and 25 show x-ray diffraction patterns of these samples. Little change of interplanar spacings is observable. However, the intensity distribution of the diffraction lines changed, indicating a possible change of crystal structure due to the loss of water. As can be seen from Fig. 24, the change is reversible. When the evacuated capillary containing the sample was exposed to air, the original diffraction pattern of the initial samples were again obtained.

A more detailed study of this effect is proceeding. However, this preliminary data has been presented simply to show that several new phases of heavy metal cyanides exist as a function of dehydration.

Dehydration-Rehydration Behavior. To summarize some of the behavior described in the above paragraphs, cupric ferrocyanide gel, exhibiting a spheroidal morphology in the electron microscope and exhibiting only standard cubic diffration lines, yields a bivarient dehydration isobar, indicating that the water content is adsorbed (on the outside of the particles or within the channels in the crystal structure) or zeolitic in character. There is no direct evidence that such water molecules are present in definite crystollographic positions. However the cupric ferrocyanide gel just described is reddish-brown in color, as opposed to the bluish color exhibited by gels strongly evacuated (with or without elevation of temperatures) or subjected to a strong dehydrating liquid such as alcohol. Furthermore, the bluish gel exhibits an x-ray diffraction

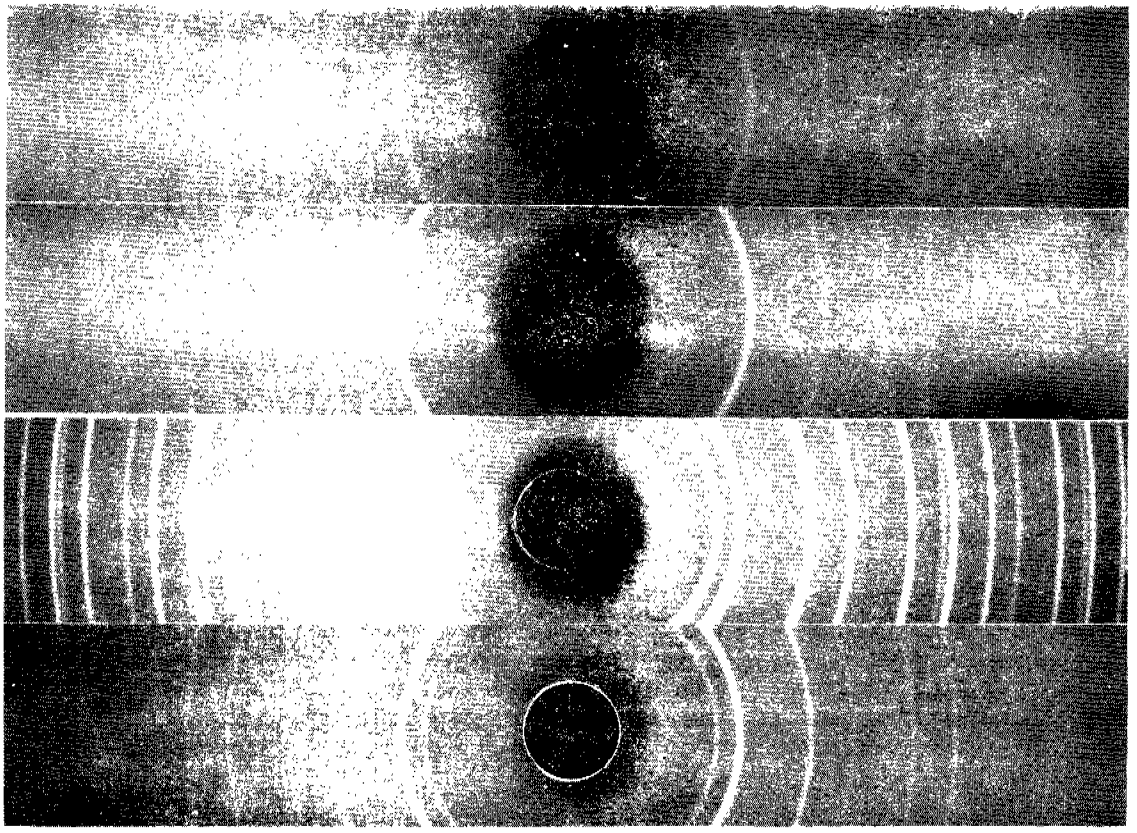

Fig. 25. X-ray diffraction patterns (Cu Kα radiation) illustrating evacuation effects of cobaltous cobalticyanide and cadmium ferricyanide: a, Fresh precipitate of cobaltous cobalticyanide; b, Sample A evacuated with fore pump for 1 hr at room temperature; c, Fresh precipitate of cadmium ferricyanide; d, Sample C evacuated with fore pump for 1.5 hrs at room temperature.

slightly different from the original reddish-brown material. This latter is especially true if the evacuation involve some heating, where decomposition reactions are likely to occur.

In this case it is important to compare the properties of the reddish-brown and the blue gels under conditions where such chemical decomposition is avoided. Possibly evacuation at low temperatures will be required.

A similar problem exists in the instance of the rose and blue forms of cobalticyanide.

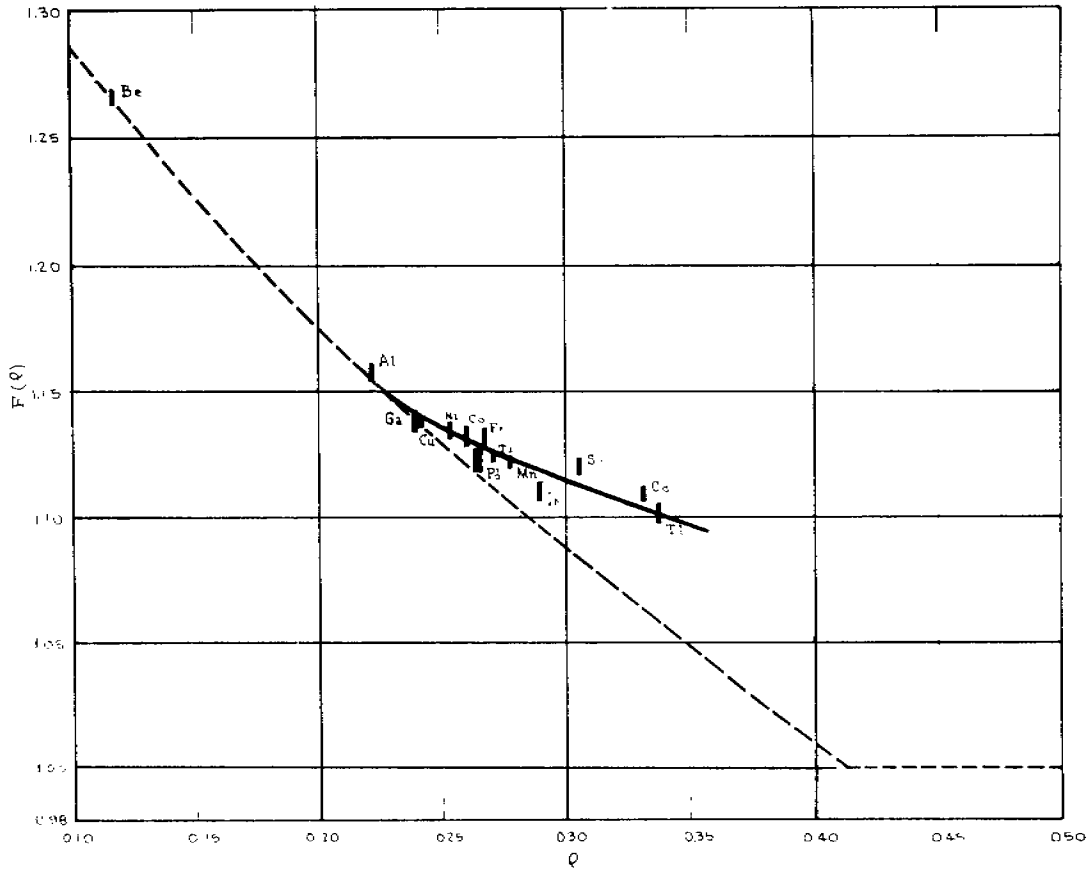

Fig. 27. Effect of radius Ratio on Interatomic Distances in Complex Cyanides.

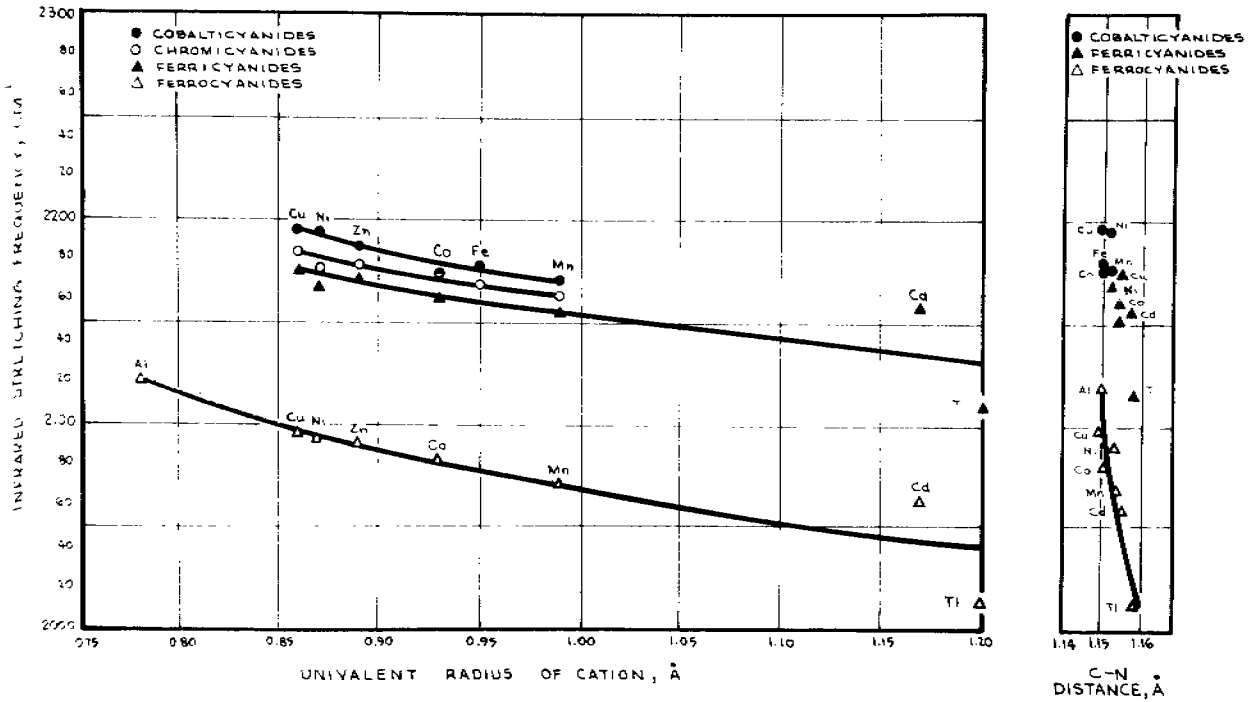

Fig. 28. Infrared Stretching Frequencies versus univalent radii of cations for reversal complex cyanides.

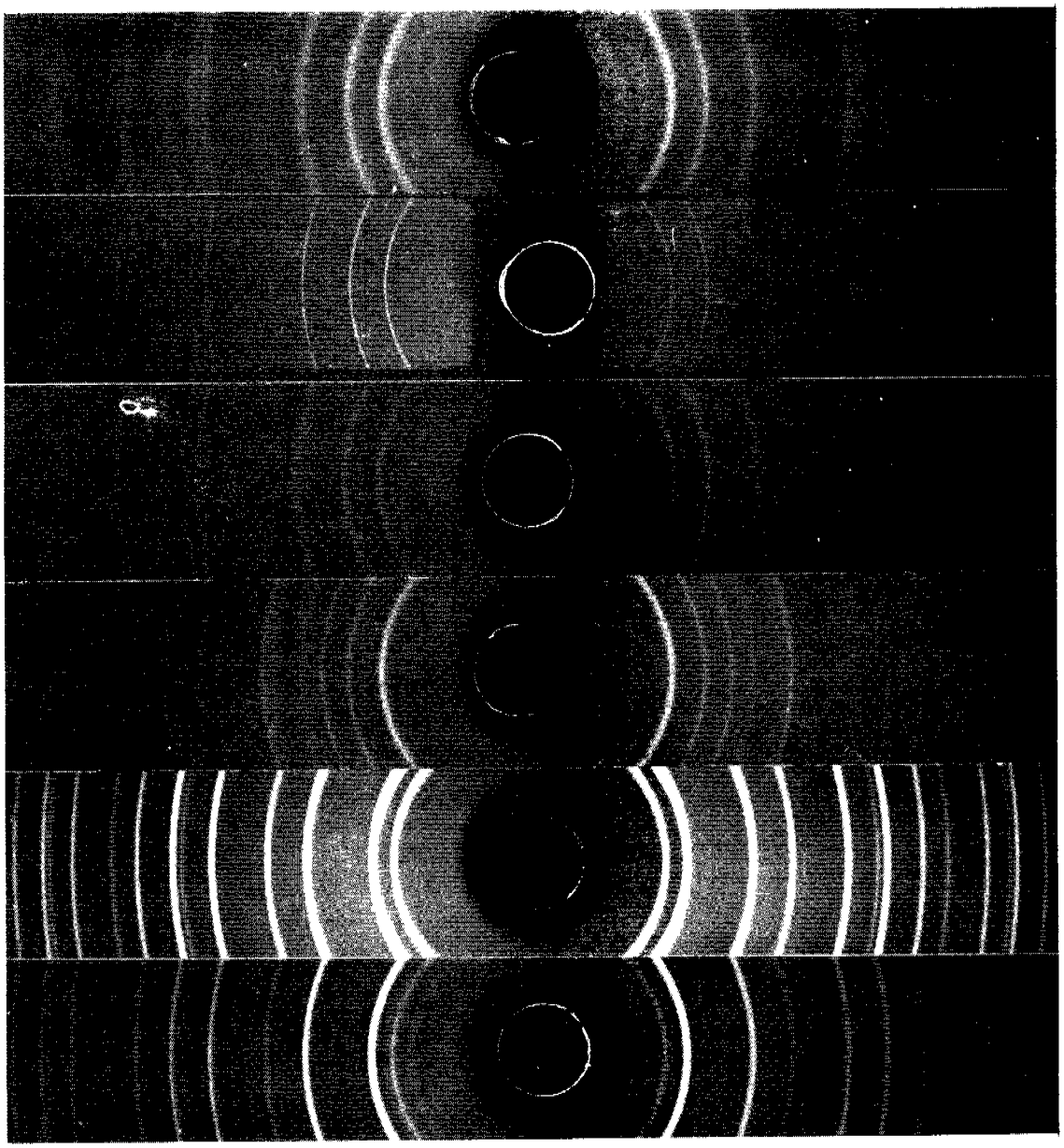

Fig. 29. X-ray diffraction patterns (Cu Kα radiation) for the following hexagonal crystals: A, thorium ferrocyanide; B, europium ferricyanide; C, europium ferrocyanide; D, europium ferrocianide with impurities; and the cubic crystals E, cadmium ferricyanide; F, cadmium ferricyanide with impurities.

Recoil-free γ-ray fluorescence spectroscopy is a logical complimentary tool with x-ray diffraction methods for structural studies, inasmuch as the former defines the charge states of the ions and the latter defines their positions.

The theory of the Mössbauer effect has been covered by several authors (90). The isomer shift is the amount by which the spectrum is shifted relative to a fixed energy (which in turn is often chosen by the experimenter as the energy emitted by his own source when at rest, but is better chosen as the center of absorption of a standard substance such as iron or sodium nitroprusside). An increased electron density at the nucleus effects a negative isomer shift. The addition of an electron to ferric iron increases the isomer shifts, however, since an added "d" electron will shield the "s" electrons and lead to a positive ismoer shift. Ferricyanide ions yield a small negative isomer shift relative to ferrocyanide, and this is part of the basis for differentiating the charged states. Shulman and Sugano (91) have preformed the MO treatments of these ions and concluded that the charge states are virtually identical. Another way of looking at it is to consider the nephelauxetic (or cloud-expanding) effect. The very strong cyanide ligands bond tightly to the iron nucleus and this shields the nonbonding t_{2g} electrons. Consequently, the absence of one of these in Fe^{III} leads to much smaller effects than occur in Fe^{3+}. This nephelauxetic effect shows up clearly in the Mössbauer effect, both in the isomer shift and in the quadrupole splitting.

Quadrupole splitting in iron compounds is caused by the interaction of the electric field gradient with the nuclear quadrupole moment (92). It is generally useless to try to visualize the electric field gradient as the gradient of the electric field at the nucleus. For one thing, the electric field at the nucleus is zero. If this were not so, the nucleus, being charged, would move to a position where the electric field was zero. Further, the gradient of a vector is a second rank tensor with nine components. It is useful to think of the electric field gradient (efg) tensor in terms of the shape of the charge distribution. If the charges are electrons, and hence negative, it is meaningful to specify that the equivalent ellipsoid of charge is spherical, football-shaped or pancake-shaped. In terms of the efg tensor, this equivalent to specifying V_{22} as zero, negative, or positive. If axial symmetry is not present, an assymmetry parameter must be introduced. The quadrupole splitting in iron compounds is complicated by the two contributions to the efg tensor; the ligands which represent localized concentration of electrons, and the 3d electrons which are nonspherical. The ligand contribution to the efg tensor of the iron cyanides is zero, by

were done in a stream of nitrogen, similar to the procedure described in the preceding paragraph.

Ferrous ferrocyanide was prepared as previously described in a nitrogen atmosphere, washed in a centrifuge ten times with distilled water, and allowed to dry under nitrogen. (This was the same procedure as for the titanium compounds except for the hydrochloric acid.)

Ferric ferricyanide was prepared in air, washed ten times with distilled water in a centrifuge at 3000 r.p.m., filtered, and air-dried.

c. Cobalt-Containing Complexes. Cobalt-containing complexes were prepared by quick mixing at room temperature dilute solutions (0.1 N) of ferrous sulfate (ACS reagent grade) with 0.1 N potassium cobalticyanide. The cobaltous ferro- and ferricyanide complexes were prepared by quick mixing at room temperature dilute solutions (0.1 N) of cobaltous chloride and the corresponding potassium ferro- and ferricyanide solutions. The resulting suspensions of the freshly precipitated cobalt-containing gels were washed ten times with distilled water in a centrifuge at 3000 r.p.m. and allowed to age under water at room temperature. These samples were allowed to age for several weeks in the hope of growing larger crystals which would give sharper x-ray diffraction lines. However, little or no detectable change occurs after a period of 6 weeks, at which time the gels were then suction-filtered using Whatman No. 42 filter paper and allowed to dry.

d. Environment with ^{57}Fe. In order to separate the severely overlapping Mössbauer spectra of Prussian blue, Trunbull's blue and ferric ferricyanide, selective enrichment of Fe^{3+} and Fe^{2+} ions in Prussian blue and Turnbull's blue, respectively, and $Fe(CN)_6^{3-}$ ion in the ferric ferricyanide was increased from its normal 2.17% ^{57}Fe to 92% ^{57}Fe, giving rise to well-defined nonoverlapping Mössbauer absorption peaks.

The enrighment was accomplished as follows. A 92% enriched $^{57}FeCl_3$ stock solution was prepared by dissolving 92% enriched $^{57}Fe_2O_3$ in excess hot hydrochloric acid. Excess hydrochloric acid was removed by repeatedly evaporating to near dryness at the boiling point and adding distilled water, until the resulting solution of $^{57}FeCl_3$ gave a pH value of about 3.

A $^{57}Fe_2(SO_4)_2$ solution was obtained by slow addition of H_2So_4 to a portion of the stock solution and evaporating to near dryness. the resulting solution was then frozen in liquid nitrogen. The

TABLE VIII PREPARATION OF SAMPLES

Sample No.	Solutions mixed: 0.1 N (5% excess)	Solutions mixed: 0.1 N	Remarks		Mossbauer spectra in figure
1[a,b]	$TiCl_3$	$H_4Fe(CN)_6$	Dried in N_2 atm		31
2[a,b]	$TiCl_3$	$H_3Fe(CN)_6$	Dried in N_2 atm		32
3[a,b]	$TiCl_4$	$H_4Fe(CN)_6$	Dried in N_2 atm		33
4[c]	$Fe_2(SO_4)_3$	$K_4Fe(CN)_6$	"Prussian blue"	undried, washed ppt frozen at 77° within 10 min after precipn step	34
5[c,d]	$Fe_2(SO_4)_3$	$K_4Fe(CN)_6$	"Prussian blue"		35
6[c,e]	$FeCl_2$	$K_3Fe(CN)_6$	"Turnbull's blue"		36
7[b]	$FeSO_4$	$K_4Fe(CN)_6$	Dried in N_2 atm		37
8	$Fe_2(SO_4)_3$	$K_3Fe(CN)_6$	Air-dried		38
9[f]	$Fe_2(SO_4)_3$	$K_3Fe(CN)_6$	Air-dried		39
10	$FeSO_4$	$K_3Co(CN)_6$	Air-dried		40-41
11	$CoCl_2$	$K_4Fe(CN)_6$	Air-dried		42
12	$CoCl_2$	$K_3Fe(CN)_6$	Air-dried		43-44

[a]In 6 N HCl to avoid possible hydrolysis to form hydrous titanium oxides. [b]Precipitated and transferred in nitrogen glove box to minimize possible air oxidation. [c]Partially protected from possible air oxidation by a nitrogen atmosphere. [d]Fe^{3+} enriched to 92% in ^{57}Fe. [e]Fe^{2+} enriched to 92% in ^{57}Fe. [f]$[Fe^{III}(CN)_6]^{3-}$ enriched to 92% in ^{57}Fe.

The C-N distances were in the range of 1.148 to 1.160 Å. Although only Debye-Scherrer data were available, the R values were in the range of 0.034 to 0.099. Preliminary x-ray studies have now been extended to some of the compounds reported here which may involve redox reactions. Some of the results are given in Table IX. It will be noted that the lattice constants fall in line with those reported for the 30 isomorphous structures. Although, it is evident that x-ray structural calculations cannot be expected to distinguish clearly between structures differing only as a result of a possible redox reaction, the present x-ray results are consistent with the Mossbauer spectra to be discussed in the next secton of this paper.

2. MOSSBAUER SPECTRA. There are given in Figures 31-43 Mössbauer spectra for the 12 samples listed in Table VIII. The isomer shifts (δ) and quadrupole splittings (Δ) are given in Table X and were determined by a computer-curve-fit program and are expressed in millimeters/second. From the Mössbauer spectrum shown in Figure 31 it may be deduced that when (sample no. 1) $TiCl_3$ is mixed with $H_4Fe(CN)_6$, the precipitate obtained is a ferricyanide, $Ti^{3+}{}_4[Fe(CN)_6{}^{4-}]_3$, giving a δshift of -0.01 relative to iron. Although this reaction appears to be straightforward, this is not the case when (sample no. 2) $TiCl_3$ is mixed with $H_3Fe(CN)_6$, as shown in the Mössbauer spectrus (Figure 32) of the resulting precipitate. Instead of obtaining the characteristic quadrupole splitting and isomeric shift for ferricyanides, the spectrum indicated ferrocyanide with no detectable ferricyanide present. This suggests a redox reaction has taken place, converting the compound to $Ti^{4+}[Fe(CN)_6]^{4-}$. The titanium (IV) ferrocyanide complex was then synthesized (sample no. 3) and its Mossbauer spectrum (Figure 33) was identical with that obtained from mixing (sample no. 2) $TiCl_3$ with $H_3Fe(CN)_6$. The ferrocyanide spectra shown in figures 34 and 35 are not caused by the $Ti^{3+}{}_4[Fe(CN)_6{}^{4-}]_3$ compound (Figure 33) since the isomer shift is different as well as the line width at half-height. The line width at half-height of $Ti^{3+}{}_4[Fe(CN)_6{}^{4-}]_3$ (0.67 vs. 0.54 mm/sec.). The origin of this difference is likely an unresolved quadrupole splitting which may be caused by the random filling of Ti^{3+} in the 8c positions surrounding each iron, and only 1.33 Ti^{3+} ions to fill them. The more positive isomer shift of the $Ti^{3+}{}_4[Fe(CN)_6{}^{4-}]_3$ compound remains unexplained as yet.

The Mössbauer spectrum obtained for (sample no. 4) Prussian blue, unenriched at either iron site, is shown in Figure 34. The overlapping spectrum of the iron sites makes interpretation extremely difficult without selective enrichment. The Fe^{3+} portion of the overlapping spectrum is shown in Figure 35 which was obtained by using (sample no 5) enriched $^{57}Fe_2(SO_4)_3$ in the formation of Prussian blue. the results indicate sample No. 5 to be ferric ferrocyanide.

TABLE X MOSSBAUER PARAMETERS

Sample No.	Compound (based on Mossbauer Spectra)	Fe^{III}		Fe^{II}		Fe^{3+}		Fe^{2+}	
		δ	Δ	δ	Δ	δ	Δ	δ	Δ
1	$Ti^{3+}_4[Fe(CN)_6]^{4-}_3$	...	...	-0.01	0	...	...	...	...
2	$Ti^{4+}[Fe(CN)_6]^{4-}$	...	...	-0.06	0	...	...	...	...
3	$Ti^{4+}[Fe(CN)_6]^{4-}$	...	...	-0.06	0	...	...	...	...
4,5	$Fe^{3+}_4[Fe(CN)_6]^{4-}_3$	...	...	-0.08	0	+0.49	0.57	...	...
6	$Fe^{3+}_4[Fe(CN)_6]^{4-}_3$	...	...	-0.07	0	+0.49	0.51	...	...
7	$Fe^{2+}_2[Fe(CN)_6]^{4-}$	...	...	-0.09	0	...	...	+1.42	3.02
8,9	$Fe^{3+}[Fe(CN)_6]^{3-}$	-0.06	0.43	...	...	+0.50	0.52	...	...
10	$Fe^{2+}_3[Co(CN)_6]^{3-}_2$								
	(M_I)	...	...	...	...	...	...	+1.27	2.81
	(M_{II})	...	...	...	...	...	...	+1.23	1.82
	298°K (M_I)	...	...	...	...	...	...	+1.13	1.76
	298°K (M_{II})	...	...	...	...	...	...	+1.11	0.97
11	$Co^{2+}_2[Fe(CN)_6]^{4-}$	...	...	-0.01	0	...	...	...	...
12	$Co^{2+}_3[Fe(CN)_6]^{3-}_2$	-0.08	0.85	...	...	...	...	...	...

[a]Isomer shifts (δ) and quadrupole splitting (Δ). The isomer shift is with res ect to the center of the six-line spectrum of natural iron at room temperature. The numerical values of δ and Δ are based on a computer curve-fit program and are expressed in mm/sec. Except when noted, all samples were examined at 77°K.

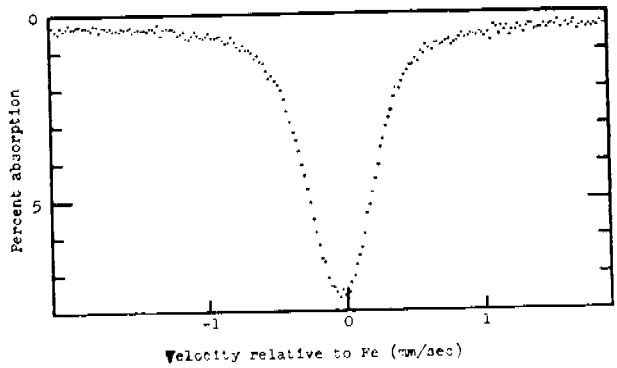

Fig. 33. Mössbauer spectrum at 77°K for $Ti^{4+}[Fe^{II}(CN)_6]^{4-}$: Sample no. 3, $TiCl_4 + H_4Fe(CN)_6$.

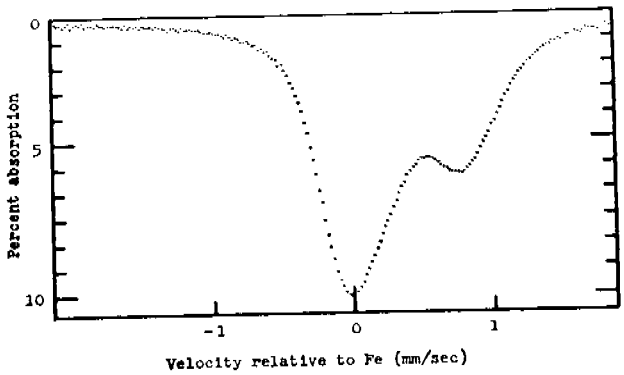

Fig. 34. Mössbauer spectrum at 77°K for $Fe^{3+}{}_4[Fe^{II}(CN)_6]^{4-}{}_3$: Sample no. 4, $Fe_2(SO_4)_3 + K_4Fe(CN)_6$, "Prussian blue."

the single ferrocyanide peak. However, even with this overlap the spectrum is easily interpreted as that of ferrous ferricyanide. In the case (sample no. 8) of Berlin green, or $FeFe(CN)_6$, the Mössbauer spectrum shown in Figure 38 suggests the two sharp peaks are due to the Fe^{3+} ion and that the $[Fe(CN)_6]^{3-}$ ion peak is hidden. This hidden ferricyanide ion peak is clearly revealed by the Mossbauer spectrum in Figure 39 where the precipitate (sample no. 9) is obtained by mixing $Fe_2(SO_4)_3$ and $K_3{}^{57}Fe(CN)_6$. The quadrupole splitting due to the ferricyanide ion is now quite visible, thus making it possible to conclude that the precipitate is ferric ferricyanide.

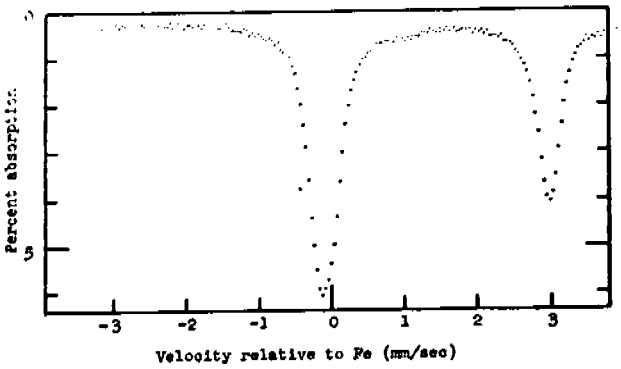

Fig. 37. Mössbauer spectrum at 77°K for $Fe^{2+}{}_2[Fe^{II}(CN)_6]^{4-}$: Sample no. 7, $FeSO_4 + K_4Fe(CN)_6$.

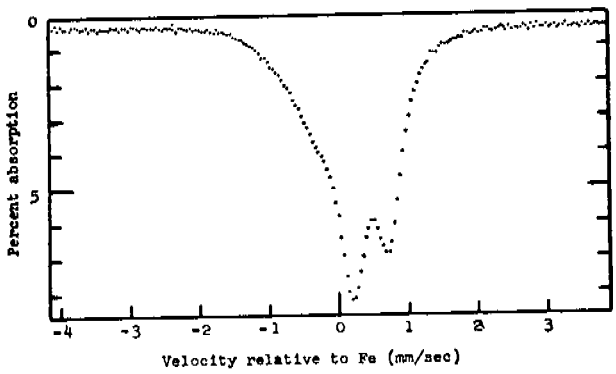

Fig. 38. Mössbauer spectrum at 77°K for $Fe^{3+}[Fe^{III}(CN)_6]^{3-}$: Sample no. 8, $Fe_2(SO_4)_3 + K_3Fe(CN)_6$.

tensors, and this accounts for the dramatic drop in quadrupole splitting as the temperature is raised. It should also be pointed out that the Fe^{2+} in the 4b positions and Fe^{2+} in the 8c positions are not equally bound (*i.e.*, not in the same environment). Interpretation of the relative intensities of the four lines in Figures 40 and 41 suggests that the inner pair of lines corresponds to the Fe^{2+} (two atoms statistically) in the 8c positions, and the outer pair of lines corresponds to the Fe^{2+} atoms in the 4b positions.

The Mössbauer spectra in Figures 42 and 43 correspond to

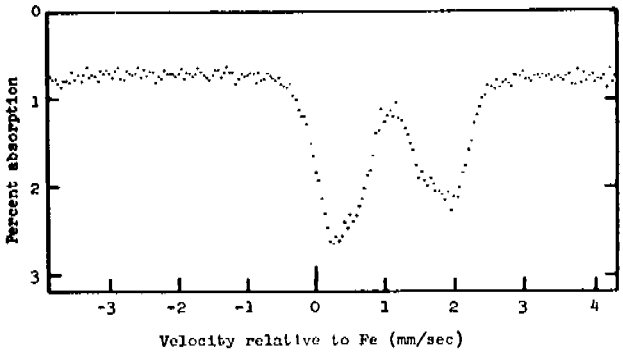

Fig. 41. Mössbauer spectrum at 298°K for $Fe^{2+}{}_3[Co^{III}(CN)_6]^{3-}{}_2$: Sample no. 10, $FeSO_4 + K_3Co(CN)_6$.

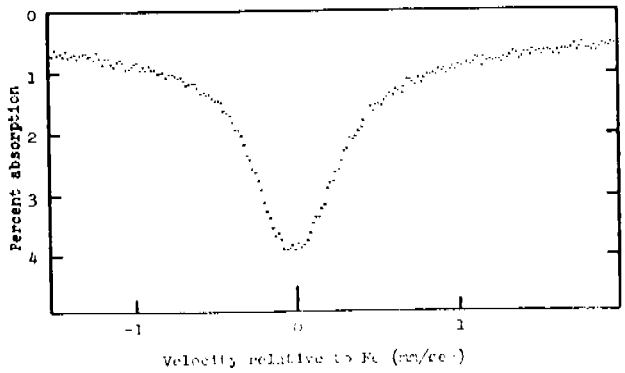

Fig. 42. Mössbauer spectrum at 77°K for $Co^{2+}{}_2[Fe^{II}(CN)_6]^{4-}$: Sample no. 11, $CoCl_2 + K_4Fe(CN)_6$.

occurs in solution, $Ti^{3+} + [Fe^{III}(CN)_6]^{3-} \rightarrow Ti^{4+} + [Fe^{II-}(CN)_6]^{4-} \rightarrow Ti^{4+}[Fe^{II}(CN)_6]^{4-}$, followed by precipitation of the insoluble $Ti^{4+}[Fe^{II}(CN)_6]^{4-}$, or whether $Ti^{3+}[Fe^{III}(CN)_6]^{3-}$ is precipitated directly from solution, followed by an internal redox reaction. $Ti^{3+}[Fe^{III}(CN)_6]^{3-} \rightarrow Ti^{4+}[Fe^{II}(CN)_6]^{4-}$. The titanium-iron cyanide complexes studied here had aged in contact with water for 6 hr. prior to acquisition of the Mössbauer spectra. In the future work it is planned to attempt to examine samples that have aged for shorter periods of time.

Furthermore, Chadwick and Sharp (99) have recently pointed out that considerations based on the formation of insoluble substances of high lattice energy and high charge may be more important than redox potentials arising from solution in determining the composition of the final product.

It appears highly desirable to develop a technique for measuring the Mössbauer spectra of the two blue gels where aging under water has been minimized.

The curve-fit program was a modification by James L. Gilchrist of J. Spijkerman's linearized least-squares curve-fit program.

VII. ACKNOWLEDGMENTS

The authors are grateful to the Office of Saline Water, Department of the Interior, for generous support of this research (Grant No. 14-01-0001-1296); to Dr. R. L. Collins and Dr. K. Maer, Jr., for their collaboration in the Mössbauer studies; to Dr. K. Kraus for helpful discussions on semi-permeability; to Dr. S. H. Simonsen for help in some x-ray intensity calculations, and to Dr. H. A. Levy and Dr. Raymond Ellison for help in x-ray intensity calculations for cadmium cobalticyanide.

VIII. REFERENCES

(1) M. Traube, Archiv. Anat. Physiol., 86 (1867).
(2) G. Tammann, Z. physik. Chem., 10, 255 (1892).
(3) P. Walden, Z. physik. Chem., 10, 699 (1892).
(4) I. Traube, Phil Mag., [6], 8, 704 (1904).
(5) P. S. Barlow, Phil. Mag., [6] 10, 1 (1905).
(6) *Cf.* L. Kahlenberg, J. Phys. Chem., 10, 169 (1906).
(7) J. Liebig, "Ursachen der Säftebewegung", (1868).
(8) J. Liebig, Liebig's Ann., 121, 78 (1862).
(9) M. L'hermite, Ann. chem. phys., [3], 43, 420 (1855).
(10) W. Nernst, Z. physik. Chem., 6, 35 (1890).
(11) E. J. Hartsung, Trans. Faraday Soc., [3], 15, 160 (1920).
(12) S. L. Bigelow, J. Am. Chem. Soc., 29, 1576, 1675 (1907); 31, 1194 (1909); J. Phys. Chem., 22, 99, 153 (1918).
(13) F. E. Bartell, J. Phys. Chem., 15, 659 (1911); 16, 318 (1912); J. Am. Chem. Soc., 36, 646 (1914); 38, 1029 1036, (1916).
(14) J. Mathieu, Ann. Physik, [4], 9, 340 (1902).
(15) A. Nathanson, Jahrb. wiss. Botan., 40 431 (1904).
(16) W. D. Bancroft, J. Phys. Chem., 21, 441 (1917).
(17) F. Tinker, Proc. Roy. Soc. (London), 92A, 357 (1916); 93A, 266 (1917).

(49) A. Ferrari and M. E. Tani, Gazz. chim. ital., 90, 1565 (1960).
(50) A. Ferrari, M. E. Tani and E. Morisi, Acta Cryst., 17, 311 (1964); 14, 695 (1961); 15, 90 (1962).
(51) A. Vaciago and A. Mugnoli, Lincei Rend. Sc. fis. mat. e nat., 25, 531-537 (1958); 26, 517-522 (1959).
(52) S. Fordham and J. T. Tyson, J. Chem. Soc., 1937, 483.
(53) W. O. Milligan and D. W. Dwight, J. Electron Microscopy (Japan), 14, 264-274 (1965).
(54) E. Lowenstein, Z. anorg. allgem. Chem., 63, 125 (1909).
(55) J. L. Culbertson, J. Am. Chem. Soc., 60, 2695 (1938).
(56) "International Tables for X-Ray Crystallography", The Kynoch Press, Birmingham, England (1952).
(57) D. T. Cromer, Acta Cryst., 18, 20 (1965).
(58) N. A. Curry and W. A. Runciman, Acta Cryst., 12, 674 (1959).
(59) A. Sequira and R. Chidambaram, Acta Cryst., 20, 910 (1966).
(60) D. F. Shriver, S. A. Shriver, and S. E. Anderson, Inorganic Chem., 5, 725-730 (1965).
(61) M. L. Beasley and W. O. Milligan, Trans. New York Acad. Sci. Ser. II. 31, 261 (1969).
(62) G. B. Seifer, Zh. Neorgan. Khim., 7, 482-486 (1962).
(63) M. U. Cohen, Rev. Sci. Instr., 6, 70 (1935).
(64) P. M. Pierrot, R. Kern, and R. Weiss, Acta Cryst., 20, 425 (1966).
(65) L. Pauling, "The Nature of the Chemical Bond", Cornell University Press, Ithaca, New York (1960).
(66) M. L. Beasley, Thesis, Baylor University (1968).
(67) H. von Mahl and W. Weitsch, Z. Naturf., A15, 1051 (1961).
(68) G. A. Bassett and A. Keller, Phil. Mag., 9 817-828 (1964).
(69) J. Samrt and R. E. Burge, Nature, 205, 1296-1297 (1965).
(70) V. Drahos and A. Delong, Nature, 209, 801-802 (1966).
(71) R. H. Wade and J. Silcox, Phys. Stat. Sol., 19, 57-76 (1967).
(72) H. B. Weiser and W. O. Milligan, J. Phys. Chem., 38, 1175-1182 (1934).
(73) H. B. Weiser, W. O. Milligan and W. C. Ekholm, J. Am. Chem. Soc., 58, 1261-1265 (1936).
(74) H. B. Weiser, and W. O. Milligan, J. Am. Chem. Soc., 59, 1456-1458 (1937).
(75) P. W. Schmidt and W. O. Milligan, J. Electronmicroscopy (Japan), 10, 238-245 (1961).
(76) K. Kanesaka, M. A. Thesis, William Marsh Rice Univ., Oct. (1963).
(77) M. S. Taggart Jr., W. O. Milligan, and H. P. Studer, Proceedings of the Third National Conference on Clays and Clay Minerals, p. 31, National Academy of Sciences-National Research Council, Washington, D. C. (1955).
(78) J. D. Hanawalt, H. W. Rinn, and L. K. Frevel, Ind. Eng. Chem. Anal. Ed., 10, 457-512 (1938).